

MgcRacGAP localized to the mitotic spindles in metaphase and accumulates to the midbody in cytokinesis.³⁶⁻³⁸ MgcRacGAP associated with microtubules through its N-terminal myosinlike domain, and overexpression of the N-terminal domain–deletion mutant or a GAP activity–defective mutant of MgcRacGAP (R385A) halted cell division and led to the formation of multinucleated cells.³⁷ Gene depletion of MgcRacGAP in mice led to death during preimplantation development caused by impaired mitosis and cytokinesis with binucleated blastomeres in which the nuclei were partially interconnected.³⁸ Thus, available data indicated that MgcRacGAP plays essential roles in the mitotic (M) phase, especially in cytokinesis, through association with the microtubules. We recently demonstrated that a serine/threonine kinase Aurora B phosphorylated MgcRacGAP at the midbody, thereby inducing its latent GAP activity toward RhoA during mitosis and that MgcRacGAP associated with RhoA on the contractile ring. We also demonstrated that the Aurora B–induced MgcRacGAP phosphorylation at Ser387 was essential for its RhoGAP activity and for the completion of cytokinesis.⁴⁰

In interphase, MgcRacGAP localizes in both the nucleus and cytoplasm, and the biologic functions of MgcRacGAP in the interphase remained elusive. Although overexpression of the antisense cDNA for MgcRacGAP efficiently inhibited the IL-6–induced differentiation of M1 cells,³¹ the underlying molecular mechanism was not clear. In this study, we demonstrate that overexpression of MgcRacGAP rendered M1 cells hyperresponsive to IL-6–induced differentiation and that MgcRacGAP and STAT3 functionally associate with each other in vivo and in vitro. Moreover, MgcRacGAP was required for the transcriptional activation of STAT3. Thus, in addition to the critical role in completion of cytokinesis in the interphase, MgcRacGAP also plays a distinct role in transcriptional activation of STAT3 in IL-6–induced differentiation of M1 cells.

Materials and methods

Culture, cytokines, and antibodies

The M1, HeLa, and 293T cells were grown in Dulbecco modified Eagle medium (DMEM) (GIBCO, Grand Island, NY) containing 10% fetal calf serum. An affinity-purified anti-MgcRacGAP antibody (Ab) was produced, as described.³⁷ The anti-Rac1 monoclonal Ab (mAb) was purchased from Transduction Laboratories (Newington, NH). The anti-Rac2 Ab, anti-STAT3 Ab (C-20), anti-STAT3 mAb (F-2), antiphospho-STAT3 Ab (B-7), anti-mitotic kinesin-like protein (anti-MKLP) Ab, and anti-hemagglutinin (anti-HA) Ab (Y-11) were obtained from Santa Cruz Biotechnology (Santa Cruz, CA). Anti-Flag (M2) mAb was purchased from Sigma (St Louis, MO). Recombinant human IL-6 and soluble IL-6R (sIL-6R) were obtained from R&D Systems (Minneapolis, MN).

Retrovirus vectors

A bicistronic retrovirus vector pMX-IRES-EGFP (pMX-IG) was constructed to transduce a gene together with an enhanced green fluorescent protein (EGFP).⁴¹ A complementary DNA for the dominant negative STAT3-Y705F (STAT3F), the Flag-tagged full-length MgcRacGAP (FL), and the deletion mutant of MgcRacGAP lacking the GAP domain (Δ GAP) or Cys domain (Δ Cys) were inserted into *EcoRI* and *NotI* sites of the pMX-IG to construct pMX-IG/STAT3F, pMX-IG/FL, pMX-IG/ Δ GAP, or pMX-IG/ Δ Cys, respectively.

Production of retrovirus and virus infection

High-titer retroviruses carrying STAT3F, FL, Δ GAP, or Δ Cys were produced in a transient retrovirus-packaging cell line PLAT-E.⁴² Briefly, PLAT-E cells were cotransfected with 3 μ g of each retrovirus vector

plasmid with the use of FuGene6 Transfection Reagent (Roche Molecular Diagnostics, Indianapolis, IN). At 48 hours after transfection, the supernatants were harvested as viral stock solutions. For infection, M1 cells (1×10^6) were incubated for 6 hours with 10 mL supernatants in the presence of 10 μ g/mL hexadimethrine bromide (Sigma). First, 10 mL fresh growth medium was added to the culture, and incubation was continued for 18 hours. The cells were resuspended with growth medium and allowed to grow for another 24 hours before the cells were sorted.

Cell sorting and flow cytometry

Briefly, 2 days after virus infection, cells were washed twice with phosphate-buffered saline (PBS) and suspended in PBS containing 1% bovine serum albumin (BSA). The infected cells were sorted on the basis of GFP expression on FACS Vantage (Becton Dickinson, San Jose, CA). The sorted cells (1×10^4) were resuspended in growth medium, and cultured for 5 days (7 days after virus infection). Half of the sorted population was used to confirm GFP expression by means of FACS Calibur (Becton Dickinson), and the other half was expanded and used for further analysis.

Immunoprecipitation and Western blotting

Immunoprecipitation, gel electrophoresis, and immunoblotting were performed as described,⁴¹ but with minor modifications. Exponentially growing cells were lysed in a buffer (0.5% Triton X-100, 50 mM Tris-HCl [tris(hydroxymethyl)aminomethane-HCl] [pH 7.5], 0.1 mM EDTA [ethylenediaminetetraacetic acid], 150 mM NaCl, 200 μ M Na_3VO_4 , 50 mM NaF, 1 mM dithiothreitol [DTT], 0.4 mM phenylmethylsulfonyl fluoride [PMSF], 3 μ g/mL aprotinin, 2 μ g/mL pepstatin A, 1 μ g/mL leupeptin) (1×10^7 per milliliter cells), and incubated on ice for 30 minutes. Cell lysates were clarified by centrifugation for 15 minutes at 12 000g prior to incubation at 4°C for 2 hours with the anti-Rac2 (or Rac1) Ab, anti-STAT3 Ab, or the control rabbit whole immunoglobulin G (IgG), and protein A–sepharose (Amersham, Arlington Heights, IL). The immunoprecipitates were subjected to sodium dodecyl sulfate–polyacrylamide gel electrophoresis (SDS-PAGE) and electrophoretically transferred onto Immobilon filters (Millipore, Billerica, MA). After blocking in a solution containing 5% BSA, the filter was probed with an anti-STAT3 Ab or anti-MgcRacGAP Ab.

Preparation of recombinant MBP-fusion proteins and MBP pull-down assays

A full-length cDNA for human MgcRacGAP (FL), either of myosin-like domain (Myo), internal domain (INT), cysteine-rich domain (Cys), or GAP domain (GAP), was inserted 3' of and in frame to the maltose binding protein (MBP) coding sequence in a bacterial expression vector pMal (New England Biolabs, Beverly, MA). Similarly, each of the murine STAT3 domains was inserted into pMal. The integrity of each coding sequence was confirmed by DNA sequencing. *Escherichia coli* BL21 (DE3) cells harboring the recombinant expression vectors were induced with 1 mM isopropyl β -D-thiogalactopyranoside (IPTG) (American Bioanalytical, Natick, MA) at 25°C for 4 hours. Cells suspended in 4 mL ice-cold suspension buffer (20 mM Tris-HCl, 200 mM NaCl, 1 mM EDTA, 1 mM DTT, and 2 mM PMSF). The cell suspension was sonicated, and insoluble debris was pelleted by centrifugation (12 000g for 15 minutes at 4°C). The supernatants were mixed with amylose resin beads (New England Biolabs) at 4°C for 30 minutes. The beads were washed 3 times and resuspended in 1 mL suspension buffer. The purity and quantity of bound MBP-fusion proteins were examined by means of SDS-PAGE followed by Coomassie blue staining. A similar amount of MBP fusion proteins bound to amylose resin beads was incubated for the time indicated with 1 mL cell lysates (1×10^7 /mL) from IL-6–stimulated (50 ng/mL) or unstimulated M1 cells. The pull-down binding reaction was done for 30 minutes at 4°C in 500 μ L binding buffer (0.5% Triton X-100, 50 mM Tris-HCl [pH 7.5], 0.1 mM EDTA, 150 mM NaCl, 5 mM MgCl_2 , 200 μ M Na_3VO_4 , 50 mM NaF, 1 mM DTT, 0.4 mM PMSF, 3 μ g/mL aprotinin, 2 μ g/mL pepstatin A, 1 μ g/mL leupeptin). The samples were resolved with the use of SDS-PAGE, followed by Western blotting with an anti-STAT3 Ab or an anti-MgcRacGAP Ab. For some experiments, the blots were stripped of bound antibodies and reprobed with anti-Rac1 mAb or anti-MKLP Ab.

Immunostaining

M1 cells, with or without stimulation of IL-6 (50 ng/mL for 12 hours), were plated on glass coverslips and fixed with 4% paraformaldehyde/PBS for 20 minutes at room temperature. The cells were then washed 3 times with ice-cold PBS followed by a 10-minute incubation at room temperature in PBS containing 0.1% Nonidet P-40. The anti-MgcRacGAP and anti-STAT3 (F-2) mAb were diluted in PBS containing 3% bovine serum albumin, placed as a drop on the coverslips, and incubated for 1 hour. The coverslips were incubated with a solution containing fluorescein isothiocyanate (FITC)-conjugated goat anti-rabbit IgG (Wako Pure Chemical Industries, Osaka, Japan) and Rhodamine-conjugated goat anti-mouse IgG (Sigma) for 1 hour. The coverslips were mounted with glycerin containing paraperylene diamine (PPD) at 10 mg/mL and 4',6-diamino-2-phenylindole (DAPI) at 1 μ g/mL for 30 minutes, then viewed by means of a fluorescence microscope IX70 (Olympus, Tokyo, Japan) equipped with SenSys/OL cold charge-coupled device (CCD) camera (Olympus) and IP-Lab software (Signal Analytics, Vienna, VA). The objective lens used was an LCPlanFI \times 40/0.60 (Olympus).

Generation, expression, and purification of MgcRacGAP recombinant protein in Sf-9 cells

The cDNA encoding MgcRacGAP with the C-terminal Flag epitope tag was subcloned into the baculovirus transfer vector pBacPAK (BD Biosciences, San Jose, CA). The resulting construct was used to acquire recombinant baculoviruses by cotransfection with Bsu36 I-digested BacPAK viral DNA (BD Biosciences) according to the manufacturer's protocol. For protein expression, Sf-9 cells were infected with high-titer viral stocks for 96 hours and lysed in lysis buffer (50 mM Tris-HCl [pH 7.5], 150 mM NaCl, 1.0% Nonidet P-40, 1 mM EDTA, 0.2 mM Na₃VO₄, 2 mM PMSF, 2 μ g/mL leupeptin, 10 μ g/mL aprotinin). The lysate was clarified by centrifugation, and the supernatant was immunoprecipitated with the anti-Flag M2-agarose-affinity gel (Sigma) for 2 hours at 4°C. The agarose beads were washed 3 times with the lysis buffer, and the recombinant MgcRacGAP was eluted with 3 \times Flag fusion protein (Sigma). To confirm the purity, the eluted MgcRacGAP was subjected to SDS-PAGE, followed by Coomassie blue staining (data not shown).

Luciferase reporter assay

HeLa cells were transfected with 0.6 μ g pME, pME/FL, pME/ Δ GAP, or pME/ Δ Cys together with 0.6 μ g reporter plasmid carrying a firefly luciferase gene driven by the glial fibrillary acidic protein (GFAP) promoter³³ and 0.6 μ g internal control reporter plasmid with the Rous sarcoma virus long-terminal repeat promoter by means of Lipofectamine Plus Reagents (Life Technologies, Bethesda, MD). At 24 hours after transfection, cells were stimulated with IL-6 (20 ng/mL) and sIL-6R (20 ng/mL) for 12 hours or left untreated before cell lysates were prepared. Cell lysates were then subjected to a dual luciferase reporter system (Promega, Madison, WI). Transfection efficiency was normalized with Renilla luciferase activity.

RNA interference for MgcRacGAP

Expression of MgcRacGAP was selectively suppressed by means of the RNA interference method, as described.³⁹ We used CCUCUUCUGACCU-UUCGCC as a target sequence of MgcRacGAP and GCCUCUUGUACU-UCCCCU as a scrambled sequence, and 293T cells were incubated with the MgcRacGAP siRNA (10 nM) with the use of Lipofectamine 2000 (Life Technologies). After 48 hours, cells were subjected to the reporter assay.

Results

Overexpression of the sense cDNA for MgcRacGAP renders M1 cells hyperresponsive to IL-6-induced macrophage differentiation

Expression of the antisense cDNA for MgcRacGAP significantly inhibited the IL-6-induced macrophage differentiation of murine

myeloid leukemia M1 cells.³¹ However, how MgcRacGAP was involved in the IL-6-mediated cellular responses was not determined. To investigate the role of MgcRacGAP in IL-6-mediated cell differentiation, we overexpressed MgcRacGAP (FL) and, as a control, a dominant negative mutant STAT3 (STAT3F) in M1 cells using pMX-IRES-GFP (pMX-IG). After transduction of M1 cells with these vectors, GFP⁺ cells were collected by means of a cell sorter, and we confirmed that most of the sorted cells expressed GFP at high levels (Figure 1A). The expression of Flag-tagged FL and HA-tagged STAT3F was also confirmed in Western blot analysis (Figure 1B). Since overexpression of the FL alone did not induce detectable differentiation of M1 cells, we asked if it renders M1 cells more sensitive to IL-6-induced differentiation. The sorted cells were cultured for 4 days in the presence of 5 ng/mL IL-6. Flow cytometric analysis was done to quantify morphologic changes that occurred after the culture. Increase in cell size and granule content of the cytoplasm were evaluated on the basis of the increase in forward scatter (FSC) and side scatter (SSC), respectively (Figure 1C). After treatment with IL-6, while 52% of M1 cells transduced with the control vector pMX-IG showed a shift from region R1 to region R2, a hallmark of macrophage differentiation, 90% of the M1 cells transduced with the control vector pMX-IG/FL showed similar shifts. Conversely, only 9% of M1 cells transduced with pMX-IG/STAT3F shifted from region R1 to region R2. To further

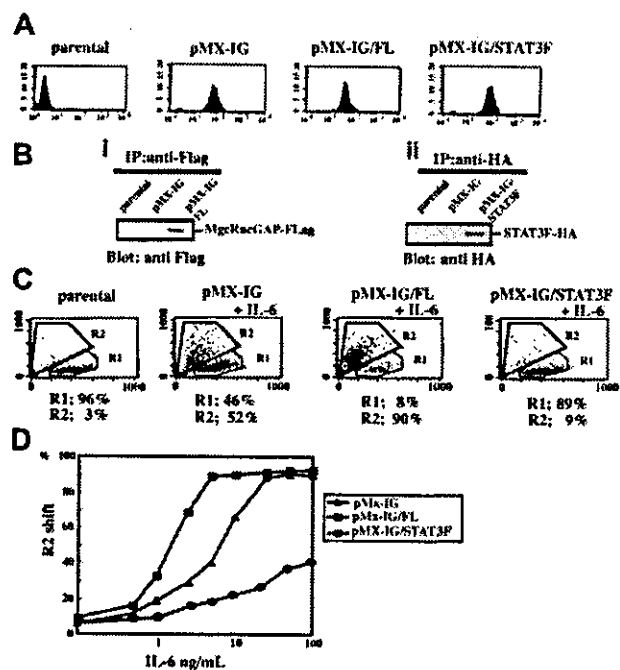
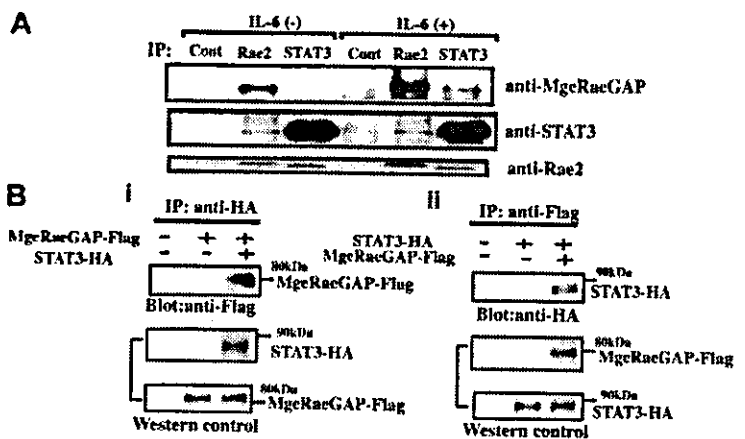


Figure 1. Effect of MgcRacGAP on M1 cell sensitivity to IL-6-induced differentiation. MgcRacGAP renders M1 cells more sensitive to the IL-6-induced differentiation signal. (A) Quantitation of GFP expression in the M1 cells at 4 days after retroviral gene transduction on flow cytometry in pMX-IG, pMX-IG/FL, or pMX-IG/STAT3F. The x-axis indicates fluorescence intensity as a log scale ranging from 10^0 to 10^4 . The y-axis indicates the number of the cells. Parental M1 cells were used as a control. (B) Expression of the Flag-tagged FL and HA-tagged STAT3F in M1 transfectants. Cell lysates from parental M1, M1/pMX-IG, and M1/pMX-IG/FL cells (1×10^7 per lane) were immunoprecipitated and examined by means of immunoblotting and an anti-Flag M2 monoclonal antibody (i). Cell lysates from parental M1, M1/pMX-IG, and M1/pMX-IG/FL cells (1×10^7 per lane) were immunoprecipitated with the use of the anti-HA monoclonal antibody (12CA5) and immunoblotted with anti-HA rabbit polyclonal Ab (ii). (C) Quantitation of cell differentiation on flow cytometry in unstimulated parental M1 cells and M1 cells expressing pMX-IG, pMX-IG/FL, or pMX-IG/STAT3F at 4 days after IL-6 treatment (5 ng/mL). Differentiated M1 cells were detected in region R2. (D) M1 cells expressing pMX-IG, pMX-IG/FL, or pMX-IG/STAT3F were incubated for 4 days with various concentrations of IL-6. The cells were then analyzed for the differentiation on flow cytometry. The percentages of differentiated cells were evaluated by the percentages of the cells in the R2 region. The result shown is representative of 3 experiments.

Figure 2. In vivo interaction of MgcRacGAP with STAT3 and Rac GTPases. (A) Coprecipitation of STAT3, MgcRacGAP, and Rac2. M1 cells were incubated in the presence or absence of 50 ng/mL IL-6 for 15 minutes, and the cell lysates were subjected to immunoprecipitation with anti-STAT3, anti-Rac2, and a control Ab, followed by the immunoblotting with anti-MgcRacGAP, anti-STAT3, or anti-Rac2 Ab. (B) (i) Coprecipitation of MgcRacGAP with STAT3 in 293T cells transfected with Flag-tagged MgcRacGAP and either the empty vector or HA-tagged STAT3. Cell lysates were immunoprecipitated with anti-HA, and immunoblotted with anti-Flag (top panel). Levels of transfected STAT3-HA and MgcRacGAP-Flag were assayed by blotting with anti-HA and anti-Flag (middle and bottom panels). Cells transfected with the empty vectors alone were used as a negative control. (ii) Coprecipitation of STAT3 with MgcRacGAP in 293T cells transfected with STAT3-HA and either the empty vector or MgcRacGAP-Flag. Cell lysates were immunoprecipitated with anti-Flag and immunoblotted with anti-HA (top panel). Levels of transfected MgcRacGAP-Flag and STAT3-HA were assayed by blotting with anti-Flag and anti-HA (middle and bottom panels). Cells transfected with the empty vector alone were also used as a negative control.



confirm the positive effect of MgcRacGAP overexpression in the induction of M1 differentiation, we also measured percentages of the cells that underwent differentiation in response to various concentrations of IL-6. Most of the M1 cells transduced with pMX-IG/FL underwent differentiation in response to 5 ng/mL IL-6, while higher concentrations of IL-6 (25 to 50 ng/mL) were required to achieve similar levels of differentiation in the control M1 cells. On the other hand, a dominant negative STAT3F potently inhibited the differentiation of M1 cells even at the higher concentrations of IL-6, up to 100 ng/mL (Figure 1D). These results indicated that the overexpression of MgcRacGAP rendered M1 cells hyperresponsive to the IL-6 and confirmed that STAT3F strongly suppressed the IL-6-induced macrophage differentiation of M1 cells, as reported.¹⁴

Rac, STAT3, and MgcRacGAP form a complex in hematopoietic M1 cells

To understand how MgcRacGAP enhanced the IL-6-induced cellular differentiation, we next sought to identify molecules interacting with MgcRacGAP in the IL-6 signaling pathway. STAT3, which plays a central role in the IL-6-induced differentiation of M1 cells,¹⁷ directly binds to Rac1,⁴⁴ and MgcRacGAP directly binds to, and serves as a GAP against Rac1, Rac2, and Cdc42 in vitro.^{31,32} Rac2 is 92% homologous to Rac1 and is highly expressed in hemopoietic cells, while Rac1 expression is ubiquitous.^{45,46} To determine if there are interactions among STAT3, Rac2, and MgcRacGAP, we performed the immunoprecipitation in M1 cells; we precipitated the endogenous proteins from M1 cells before and after IL-6 stimulation with anti-STAT3 Ab, anti-Rac2 Ab, or a control Ab. Both STAT3 and MgcRacGAP were coimmunoprecipitated with Rac2 in the cell lysate of M1 cells with or without IL-6 (Figure 2A). We also confirmed that STAT3 and MgcRacGAP coimmunoprecipitated with Rac1 (data not shown). In addition, MgcRacGAP coimmunoprecipitated with STAT3 in the cell lysate of M1 cells stimulated with IL-6. While the pre-existing association between MgcRacGAP and Rac2 was enhanced by IL-6, the association between MgcRacGAP and STAT3 seemed to be IL-6 dependent (Figure 2A). To confirm the binding using a different set of antibodies, 293T cells were transfected with Flag-tagged MgcRacGAP and either HA-tagged STAT3 or a control vector. Flag-tagged MgcRacGAP was found in anti-HA immunoprecipitates when HA-tagged STAT3 was coexpressed (Figure 2Bi, upper panel); conversely, HA-tagged STAT3 was detected in anti-Flag immunoprecipitates when Flag-tagged MgcRacGAP was coexpressed (Figure 2Bii, upper panel). All together, these results demonstrated that STAT3 and MgcRacGAP associated with each other in vivo.

Delineation of the regions of MgcRacGAP and STAT3 that mediate their interaction

To map the interacting domains of MgcRacGAP with STAT3, we made a series of truncation constructs or FL of MgcRacGAP fused with MBP (Figure 3A), and performed the pull-down assay. Similar amounts of MBP-MgcRacGAP fusion proteins bound to amylose resin beads (Figure 3B) were incubated with cell lysates of the IL-6-stimulated M1 cells (50 ng/mL IL-6 for 30 minutes), and the retained proteins were analyzed by immunoblotting with anti-STAT3 Ab and anti-Rac1 Ab. Both STAT3 and Rac1 bound to the

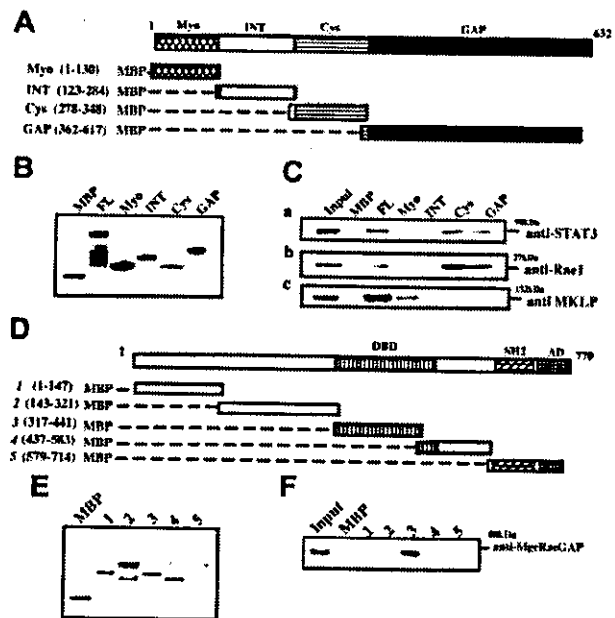


Figure 3. MgcRacGAP interactions at the Cys-rich and GAP domains with the DNA-binding domains of STAT3. STAT3 and Rac1 interact with MgcRacGAP at the Cys-rich domain and GAP domain, while MgcRacGAP interacts with the DNA-binding domain of STAT3. (A) Schematic diagram of various MBP-MgcRacGAP fusion proteins. (B) Purity and quantity of MBP and various MBP-MgcRacGAP fusion proteins were examined by means of SDS-PAGE followed by Coomassie blue staining. (C) Two regions required for MgcRacGAP-STAT3 and MgcRacGAP-Rac1 interactions. Lysates from IL-6-treated M1 (50 ng/mL for 30 minutes) were incubated with similar amounts of different MBP or MBP-MgcRacGAP fusion proteins bound to beads. Bound proteins were separated on SDS-PAGE and immunoblotted with anti-STAT3 Ab (i), anti-Rac1 Ab (ii), or anti-MKLP Ab (iii). (D) Schematic diagram of various MBP-STAT3 truncations. DBD and AD represent DNA-binding domain and activation domain, respectively. (E) The purity and quantity of MBP and various MBP-STAT3 truncations were examined by means of SDS-PAGE followed by Coomassie blue staining. (F) A region required for STAT3-MgcRacGAP interaction. Lysates from IL-6-treated M1 (50 ng/mL for 30 minutes) were incubated with a similar amount of different MBP or MBP-STAT3 truncations bound to beads. Bound proteins were separated on SDS-PAGE and immunoblotted with anti-MgcRacGAP Ab.

Cys and GAP domain as well as the FL of MgcRacGAP (Figure 3Ci-ii). MKLP, which interacts with the Myo domain (Myo) of MgcRacGAP,³⁹ was used as a positive control (Figure 3Ciii). We next sought to define the binding domain of STAT3 to MgcRacGAP and prepared MBP-fused STAT3 truncations (Figure 3D). A similar amount of MBP-STAT3 truncations bound to beads (Figure 3E), and it was clear that DBD of STAT3 bound MgcRacGAP under a stringent condition using 0.5% Triton-X (Figure 3F). The activation domain of STAT3 could also weakly bind MgcRacGAP in a nonstringent condition using 0.1% Triton-X (data not shown). These results raise a possibility that both MgcRacGAP and STAT3 harbor 2 domains interacting with each other.

Augmentation of the association of MgcRacGAP with STAT3 upon IL-6 stimulation

We next studied the kinetics of association between STAT3 and MgcRacGAP upon IL-6 stimulation using the MBP pull-down assay. The amount of STAT3 bound to the Cys and GAP domains of MgcRacGAP apparently increased upon IL-6 stimulation (Figure 4Ai). The amount of Rac1 bound to the same domains of MgcRacGAP also increased upon IL-6 stimulation (Figure 4Aii). These results suggested that MgcRacGAP bound STAT3 without IL-6 stimulation but that the binding was enhanced by IL-6 stimulation. To further confirm the cytokine-dependent augmentation of the interaction, we visualized MgcRacGAP and STAT3 in the M1 cells before and after the IL-6 stimulation using anti-STAT3 mAb and anti-MgcRacGAP Ab (Figure 4B). As shown in Figure 4Biv, MgcRacGAP and STAT3 partly colocalized in the cytoplasm

of the unstimulated M1 cells. However, upon IL-6 stimulation, most STAT3 translocated to the nucleus, and a part of MgcRacGAP moved into the nucleus (Figure 4Bv-vi), resulting in colocalization of MgcRacGAP and STAT3 with a speckled pattern (Figure 4Bviii). Small insets to Figure 4Biv and 4Bviii showed the better details of colocalization of MgcRacGAP and STAT3 in the cytoplasm and nucleus. To confirm that the association between MgcRacGAP and STAT3 is direct, we produced and purified a Flag-tagged MgcRacGAP in Sf-9 cells and performed the pull-down assay. We found that the purified MgcRacGAP was pulled down by the MBP-STAT3-DBD but not by MBP alone, indicating that MgcRacGAP directly bound STAT3 (Figure 4C). Interaction of STAT3 with both Rac1 and MgcRacGAP was further confirmed with the use of a yeast 2-hybrid system (data not shown). Therefore, it is most likely that Rac, MgcRacGAP, and STAT3 interact directly with each other in a noninterdependent manner.

MgcRacGAP enhances the transactivation of STAT3, and the GAP domain is required for the enhancement

To determine if MgcRacGAP could alter the transcriptional activation of STAT3, we did the luciferase assay. HeLa cells were cotransfected with the luciferase reporter,⁴³ the internal control, and a vector carrying the full-length wild-type MgcRacGAP with a Flag-tag (FL), the GAP domain deletion mutant (Δ GAP), the cysteine-rich domain deletion mutant (Δ Cys), or the vector alone (Mock) (Figure 5A). Flag tag did not affect the Rac-GAP activity of MgcRacGAP, and deletion of the GAP domain abolished the GAP activity (data not shown). As shown in Figure 5B, the IL-6-induced

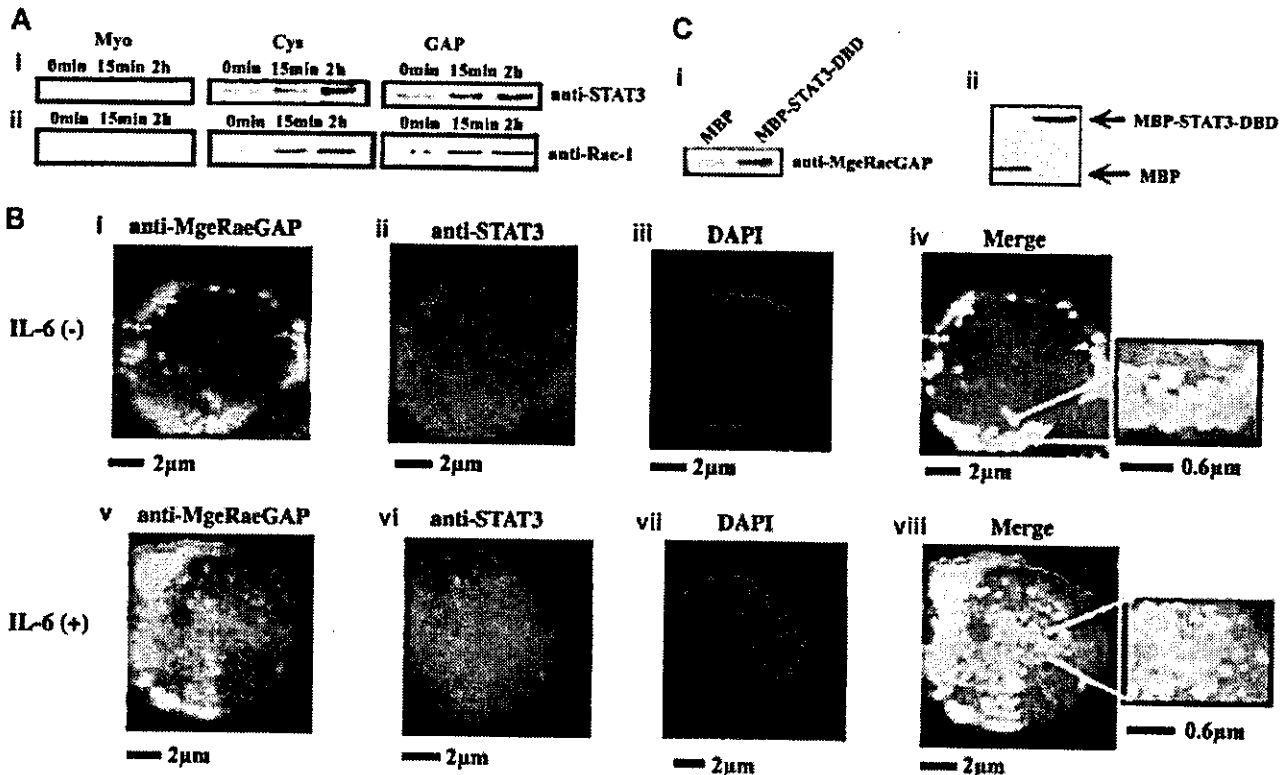
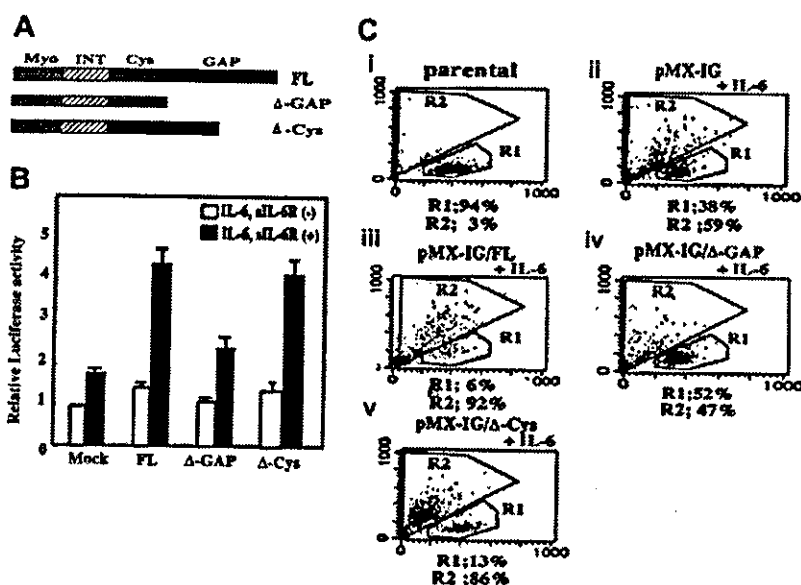


Figure 4. Enhancement of MgcRacGAP-STAT3 interaction by IL-6 stimulation. (A) Lysates from IL-6-stimulated M1 cells (50 ng/mL for the time indicated) were incubated with a similar amount of MBP-Myo, MBP-Cys, or MBP-GAP bound to beads. Bound proteins were separated on SDS-PAGE and immunoblotted with anti-STAT3 Ab or anti-Rac1 Ab. (B) MgcRacGAP partially colocalized with STAT3 at the cytoplasm and at the nucleus in M1 cells. With the use of unstimulated (i-iv) and IL-6-stimulated (v-viii) M1 cells, immunostaining for MgcRacGAP (i,v) and STAT3 (ii,vi) was done. For the merge figures (iv,viii), small insets on the right show the field at a high magnification to demonstrate the detail of the colocalization of MgcRacGAP and STAT3. The immunostained coverslips were viewed with a fluorescence microscope IX70 (Olympus). The scale bar indicates 2 μ m or 0.6 μ m. (C) Direct interaction of MgcRacGAP with STAT3-DNA-binding domain in vitro. Full-length MgcRacGAP was expressed in Sf9 cells with the use of the baculovirus vector and was purified from infected Sf9 cells. The recombinant MgcRacGAP was pulled down by MBP-STAT3-DBD- or MBP-bound beads, then subjected to Western blot analysis with anti-MgcRacGAP (i) or anti-MBP Ab for the loading control (ii).

Figure 5. Requirement of the GAP domain in the MgcRacGAP enhancement of IL-6-mediated STAT3 activation in HeLa cells and differentiation of M1 cells. The GAP domain is required for augmentation of IL-6-mediated STAT3 transactivation in HeLa cells and for IL-6-induced differentiation of M1 cells. (A) The structures of FL and deletion mutants of MgcRacGAP lacking the GAP domain (Δ GAP) or the cysteine-rich domain (Δ Cys). (B) The Δ GAP did not augment the IL-6-mediated transactivation of STAT3. Luciferase activities were examined in lysates of unstimulated or IL-6- and siL-6R-stimulated HeLa cells cotransfected with the internal control reporter plasmids and either the mock vector (pME) or the expression vector for the FL, Δ GAP, or Δ Cys as described in "Materials and methods." The results shown are the averages \pm standard deviations of 3 independent experiments. (C) Quantification of cell differentiation on flow cytometry in untreated parental M1 (i), and in M1 cells expressing pMX-IG (ii), pMX-IG-FL (iii), pMX-IG- Δ GAP (iv), or pMX-IG- Δ Cys (v) at 4 days after IL-6 treatment (5 ng/mL). Differentiated M1 cells were detected in region R2.



activation of STAT3 was enhanced by cotransfection with FL (approximately 4.5-fold) and Δ Cys (approximately 4.0-fold) (Figure 5B). However, cotransfection of Δ GAP did not significantly enhance the IL-6-induced transactivation of STAT3. Thus, the GAP domain, but not the Cys domain, was required for the MgcRacGAP-mediated enhancement of IL-6-induced transcriptional activation of STAT3.

The GAP domain of MgcRacGAP is required to render M1 cells hyperresponsive to IL-6-induced macrophage differentiation

Since overexpression of the MgcRacGAP rendered M1 cells hypersensitive to IL-6, we next investigated whether overexpression of Δ GAP or Δ Cys could alter the IL-6 sensitivity of M1 cells. The Δ GAP and Δ Cys mutants were expressed in M1 cells via retrovirus infection. As a positive and negative control, respectively, pMX-IG/FL and pMX-IG alone were also introduced into M1 cells. After infection of M1 cells with these vectors, the GFP⁺ cells were sorted on a fluorescence-activated cell sorter (FACS). We confirmed that the sorted GFP⁺ M1 cells expressed the Flag-tagged FL and mutants of MgcRacGAP at similar levels using Western blot analysis (data not shown). The sorted cells were cultured for 4 days in the presence of 5 ng/mL IL-6, and the cell differentiation was evaluated by flow cytometric analysis. Consistent with the results in Figure 1B, 59% of M1 cells transduced with the control vector pMX-IG showed a shift from region R1 to region R2. On the other hand, over 90% of the M1 cells transduced with pMX-IG/FL and 86% of those transduced with pMX-IG/ Δ Cys showed differentiation (shift from R1 to R2) (Figure 5Ciii, 5Cv). Only 47% of M1 cells transduced with Δ GAP showed the shift (Figure 5Civ), indicating that Δ GAP did not significantly enhance the sensitivity of M1 cells to IL-6. These results paralleled the transcriptional activation of STAT3 when FL, Δ GAP, and Δ Cys were overexpressed in the luciferase assay (Figure 5B).

MgcRacGAP is required for the transcriptional activation of STAT3

Finally, we asked if MgcRacGAP is essential for the transcriptional activation of STAT3. To this end, we used siRNA to knock down MgcRacGAP in 293T cells and performed the STAT3 reporter assay using the siRNA-treated cells. As shown in Figure 6A, the IL-6-induced transcriptional activation of STAT3 was profoundly suppressed by pretreatment of the cells with siRNA for MgcRac-

GAP, compared with those with the control siRNA (approximately 0.4-fold). We confirmed that the expression levels of MgcRacGAP protein were suppressed by siRNA for MgcRacGAP (Figure 6B, upper panel), but did not alter those of β -tubulin (Figure 6B, lower panel). The siRNA suppression of MgcRacGAP also attenuated IL-6-induced transcriptional activation of STAT3 in HeLa and Huh-7 cells (approximately 0.5-fold and approximately 0.6-fold, respectively), and expression of MgcRacGAP, but not STAT3, selectively decreased in these cells (data not shown). Thus, MgcRacGAP seems to play a critical role in IL-6-induced transcriptional activation of STAT3.

Discussion

As we earlier noted, the antisense MgcRacGAP profoundly inhibited the IL-6-induced macrophage differentiation of M1 cells.³¹ We and others later demonstrated that MgcRacGAP plays a critical role in cytokinesis.^{36,37} It was known that RhoA and serine/threonine kinase

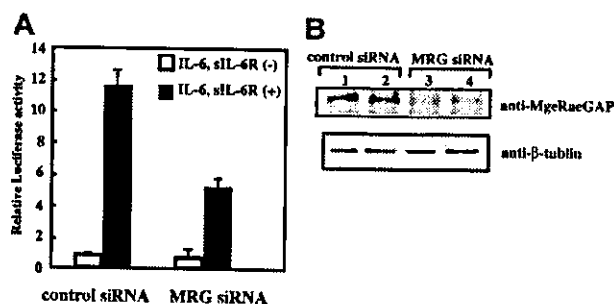


Figure 6. Suppression of STAT3-mediated transactivation by siRNA treatment for MgcRacGAP. (A) Luciferase activities were examined in the lysates of unstimulated or IL-6- and siL-6R-stimulated 293T cells with pretreatment with siRNA for MgcRacGAP (right columns) or a control siRNA (left columns). At 24 hours after the siRNA treatment, the cells were transfected with the STAT3 reporter and internal control with Lipofectamine plus reagents. Another 24 hours after the transfection, cells were stimulated with IL-6 (20 ng/mL) and siL-6R (20 ng/mL) for 12 hours before the cell lysates were prepared. The lysates were then subjected to a dual luciferase assay system, as described in "Materials and methods." The error bars show the standard deviations of triplicates. The results shown are a representative result of 3 independent experiments. (B) Expression of MgcRacGAP (upper panel) and β -tubulin (lower panel) were examined in unstimulated (lanes 1 and 3) or IL-6/siL-6R-stimulated (lanes 2 and 4) 293T cells pretreated with a control siRNA (lanes 1 and 2) or siRNA for MgcRacGAP (lanes 3 and 4) were examined.

Aurora B play important roles in cytokinesis. We have recently clarified a molecular mechanism by which MgcRacGAP controls cytokinesis; MgcRacGAP is phosphorylated at Ser387 by Aurora B at the midbody and acquires RhoGAP activity for the completion of cytokinesis.⁴⁰ However, the molecular mechanism by which MgcRacGAP affected IL-6-induced cell differentiation was still unclear. In the present work, we demonstrated that MgcRacGAP plays a role in STAT3 activation, thereby enhancing IL-6-induced differentiation of M1 cells, on the basis of the following: (1) MgcRacGAP directly bound STAT3 and Rac1/Rac2, and this interaction was enhanced by IL-6 stimulation. (2) Overexpression of MgcRacGAP rendered M1 cells hypersensitive to IL-6 stimulation, resulting in enhanced differentiation of M1 cells. (3) MgcRacGAP enhanced STAT3-induced transcriptional activation in a luciferase assay. (4) Knockdown of MgcRacGAP by siRNA profoundly inhibited STAT3-induced transcriptional activation in 293T, HeLa, and Huh-7 cells. Thus, while we and others reported that MgcRacGAP plays critical roles in cell division,^{36,37,40} the present results revealed an unexpected role for MgcRacGAP as a regulator of STAT3-mediated transcription in interphase.

GAPs for Rho GTPases constitute a class of regulatory proteins that can bind GTP-bound active forms of small G proteins and stimulate GTP hydrolysis.^{47,48} With this catalytic function, Rho-GAPs negatively regulate Rho-mediated signals. On the other hand, we demonstrated herein that the GAP domain was required for IL-6-induced STAT3 activation. It is possible that MgcRacGAP serves as an effector molecule toward Rac-STAT3 complex in the IL-6 signaling pathway. For instance, certain GAPs, including p120RasGAP, *n*-chimaerin, and phospholipase C (a GAP for heterotrimeric G proteins), simultaneously function as effectors downstream of the GTPases.⁴⁹⁻⁵¹

Concerning the cross-talk between STAT3 and a small GTPase Rac1, several groups suggested an indirect connection, and one indicated direct interaction.^{44,52,53} A constitutively active mutant RacV12 was reported to mediate STAT3 activation by autocrine IL-6 through the activation of nuclear factor- κ B (NF- κ B).⁵² It was also reported that in response to growth factor and cytokine stimulation, the activated Rac1 mediated generation of reactive oxygen species (ROS), which activated Src and JAKs, leading to STAT3 activation.^{48,53-55} In addition to the indirect connection between Rac and STAT3, it was reported that STAT3 bound directly to active but not inactive Rac1.⁴⁴ In this case, expression of RacV12 induced both tyrosine and serine phosphorylation of STAT3, whereas overexpression of a dominant negative RacN17 inhibited either tyrosine or serine phosphorylation of STAT3 induced by epidermal growth factor. However, it was not determined whether the molecular mechanism by which Rac1 induced phosphorylation of STAT3 was dependent on Rac-STAT3 interaction; tyrosine phosphorylation of JAK2 was also induced by RacV12 in their system. Gu et al⁵⁶ recently reported that Rac2 regulated transcriptional activation of c-Jun via activation of c-Jun N-terminal kinases (JNKs). Obviously, pleiotropic functions of Rac in the STAT3 activation pathway make it difficult to elucidate the biologic significance of STAT3-Rac interaction. Demonstration of the MgcRacGAP-Rac-STAT3 complex and identification of MgcRacGAP as an important regulator of STAT3 function provides

new evidence for the cross-talk between STAT3 and Rac GTPases through direct interaction.

Although we observed that RacV12 enhanced the transcriptional activation of STAT3 induced by IL-6 and sIL-6R in HeLa cells but that RacN17 suppressed it (data not shown), we have been unable to identify the underlying mechanisms involved in the enhancement of STAT3 activation by MgcRacGAP. It is possible that MgcRacGAP plays some role in nuclear transport of STAT3. In fact, MgcRacGAP partly colocalized with STAT3 in the cytoplasm without cytokine stimulation, and in the nucleus upon cytokine stimulation, showing a speckled pattern (Figure 4Bviii). Alternatively, MgcRacGAP may somehow stabilize the STAT3-DNA complex, resulting in prolonged activation of STAT3, or may work as a scaffold protein that bridges between STAT3 and unidentified transcriptional coactivators. Interestingly, in a search for proteins that interact with MgcRacGAP using the yeast 2-hybrid screening system, we recently identified a transcriptional coactivator of activating protein-1 (AP-1) and estrogen receptors (CAPER), (Y. Minoshima, T. Kawashima, and T. Kitamura, unpublished results, 2004).

Although both GAP and Cys domains of MgcRacGAP can interact with STAT3, the deletion of the Cys domain did not significantly affect MgcRacGAP-mediated enhancement of IL-6-induced transcriptional activation of STAT3 (Figure 5B) and macrophage differentiation (Figure 5C). Our results suggested that Cys domain of MgcRacGAP is dispensable for IL-6-induced transcriptional activation of STAT3 and cell differentiation. The fact that the GAP domain of MgcRacGAP was required for the enhancement of STAT3-dependent transcription (Figure 5B) and IL-6-induced cell differentiation (Figure 5C) suggests that these functions of MgcRacGAP were mediated through Rho-family small GTPases. Coordinated activation and inactivation of small GTPases by GAPs and exchange factors (GEFs) are important in exerting their biologic functions. During M phase, MgcRacGAP and epithelial cell transforming sequence 2 (ECT2) oncogene proteins colocalize and orchestrate to control cell division.⁵⁷ In addition, it has been reported that RacGAP50C, an ortholog of MgcRacGAP, binds pebble (PBL), an ortholog of ECT2, in drosophila cells⁵⁸ although the direct interaction between MgcRacGAP and ECT2 was not detectable in mammalian cells (Y. Minoshima, T. Kawashima, and T. Kitamura, unpublished results, 2004). Therefore, it is possible that ECT2 also plays some role in transcriptional activation of STAT3. Although STAT3-dependent transcription was not affected by the overexpression of ECT2 (data not shown), this may be because ECT2 requires phosphorylation to be activated. The underlying mechanism of how MgcRacGAP regulates STAT3-induced gene expression awaits further investigation; however, the present data do reveal cross-talk between small GTPases and STAT3 downstream of IL-6 receptors in which MgcRacGAP plays pivotal roles. It is tempting to postulate that MgcRacGAP controls cell proliferation and differentiation in concert with the members of Rho-family GTPase by playing dual roles in M phase and interphase, completion of cytokinesis, and regulation of transcription.

Acknowledgments

We thank M. Itoh for excellent sorting on FACS; M. Ohara for language assistance; and T. Satoh for helpful discussions.

References

1. Schindler C, Darnell JE Jr. Transcriptional responses to polypeptide ligands: the JAK-STAT pathway. *Annu Rev Biochem.* 1995;64:621-651.
2. Leonard WJ, O'Shea JJ. Jaks and STATs: biological implications. *Annu Rev Immunol.* 1998;16:293-322.
3. Ihle JN. The Stat family in cytokine signaling. *Curr Opin Cell Biol.* 2001;13:211-217.
4. Darnell JE Jr, Kerr IM, Stark GR. Jak-STAT pathways and transcriptional activation in response to IFNs and other extracellular signaling proteins. *Science.* 1994;264:1415-1421.
5. Barasch J, Yang J, Ware CB, et al. Mesenchymal to epithelial conversion in rat metanephros is induced by LIF. *Cell.* 1999;99:377-386.
6. Boccaccio C, Ando M, Tamagnone L, et al. Induction of epithelial tubules by growth factor HGF depends on the STAT pathway. *Nature.* 1998;391:285-288.
7. Bonni A, Sun Y, Nadal-Vicens M, et al. Regulation

- of gliogenesis in the central nervous system by the JAK-STAT signaling pathway. *Science*. 1999;278:477-483.
8. Bromberg JF, Wrzeszczynska MH, Devgan G, et al. Stat3 as an oncogene. *Cell*. 1999;98:295-303.
 9. Garcia R, Jove R. Activation of STAT transcription factors in oncogenic tyrosine kinase signaling. *J Biomed Sci*. 1998;5:79-85.
 10. Sano S, Itami S, Takeda K, et al. Keratinocyte-specific ablation of Stat3 exhibits impaired skin remodeling, but does not affect skin morphogenesis. *EMBO J*. 2000;18:4657-4668.
 11. Takeda K, Clausen BE, Kaisho T, et al. Enhanced Th1 activity and development of chronic enterocolitis in mice devoid of Stat3 in macrophages and neutrophils. *Immunity*. 1999;10:39-49.
 12. Shimozaki K, Nakajima K, Hirano T, Nagata S. Involvement of STAT3 in the granulocyte colony-stimulating factor-induced differentiation of myeloid cells. *J Biol Chem*. 1997;272:25184-25189.
 13. Minami M, Inoue M, Wei S, et al. STAT3 activation is a critical step in gp130-mediated terminal differentiation and growth arrest of a myeloid cell line. *Proc Natl Acad Sci U S A*. 1996;93:3963-3966.
 14. Nakajima K, Yamanaka Y, Nakae K, et al. A central role for Stat3 in IL-6-induced regulation of growth and differentiation in M1 leukemia cells. *EMBO J*. 1996;15:3651-3658.
 15. Niwa H, Burdon T, Chambers I, Smith A. Self-renewal of pluripotent embryonic stem cells is mediated via activation of STAT3. *Genes Dev*. 1998;12:2048-2060.
 16. Ernst M, Novak U, Nicholson SE, Layton JE, Dunn AR. The carboxyl-terminal domains of gp130-related cytokine receptors are necessary for suppressing embryonic stem cell differentiation. *J Biol Chem*. 1999;274:9729-9737.
 17. Taga T, Kishimoto T. Gp130 and the interleukin-6 family of cytokines. *Annu Rev Immunol*. 1997;15:797-819.
 18. Coffey PJ, Koenderman L, de Groot RP. The role of STATs in myeloid differentiation and leukemia. *Oncogene*. 2000;19:2511-2522.
 19. Matsuda T, Nakamura T, Nakao K, et al. STAT3 activation is sufficient to maintain an undifferentiated state of mouse embryonic stem cells. *EMBO J*. 1999;18:4261-4269.
 20. Benekil M, Baer MR, Baumann H, Wetzler M. Signal transducer and activator of transcription proteins in leukemias. *Blood*. 2003;101:2940-2954.
 21. Starr R, Willson TA, Viney EM, et al. A family of cytokine-inducible inhibitors of signalling. *Nature*. 1997;387:917-921.
 22. Endo TA, Masuhara M, Yokouchi M, et al. A new protein containing an SH2 domain that inhibits JAK kinases. *Nature*. 1997;387:921-924.
 23. Naka T, Narazaki M, Hirata M, et al. Structure and function of a new STAT-induced STAT inhibitor. *Nature*. 1997;387:924-929.
 24. Chung CD, Liao J, Liu B, et al. Specific inhibition of Stat3 signal transduction by PIAS3. *Science*. 1997;278:1803-1805.
 25. Rodel B, Tavassoli K, Karsunky H, et al. The zinc finger protein Gfi-1 can enhance STAT3 signaling by interacting with the STAT3 inhibitor PIAS3. *EMBO J*. 2000;19:5845-5855.
 26. Schaefer TS, Sanders LK, Nathans D. Cooperative transcriptional activity of Jun and Stat3 beta, a short form of Stat3. *Proc Natl Acad Sci U S A*. 1995;92:9097-9101.
 27. Zhang X, Zhang I, Wrzeszczynska MH, Horvath CM, Darnell JE Jr. Interacting regions in Stat3 and c-Jun that participate in cooperative transcriptional activation. *Mol Cell Biol*. 1999;19:7138-7146.
 28. Nakashima K, Yanagisawa M, Arakawa H, et al. Synergistic signaling in fetal brain by STAT3-Smad1 complex bridged by p300. *Science*. 1999;284:479-482.
 29. Lufe C, Ma J, Huang G, et al. GRIM-19, a death-regulatory gene product, suppresses Stat3 activity via functional interaction. *EMBO J*. 2003;22:1325-1335.
 30. Nakayama K, Kim KW, Miyajima A. A novel nuclear zinc finger protein EZ1 enhances nuclear retention and transactivation of STAT3. *EMBO J*. 2002;21:6174-6184.
 31. Kawashima T, Hirose K, Satoh T, et al. MgcRacGAP is involved in the control of growth and differentiation of hematopoietic cells. *Blood*. 2000;96:2116-2124.
 32. Toure A, Dorseuil O, Morin L, et al. MgcRacGAP, a new human GTPase-activating protein for Rac and Cdc42 similar to *Drosophila* rotund RacGAP gene product, is expressed in male germ cells. *J Biol Chem*. 1998;273:6019-6023.
 33. Ridley AJ. Rho family proteins: coordinating cell responses. *Trends Cell Biol*. 2001;11:474-477.
 34. Etienne-Manneville S, Hall A. Rho GTPases in cell biology. *Nature*. 2002;420:629-635.
 35. Sahai E, Marshall CJ. RHO-GTPases and cancer. *Nat Rev Cancer*. 2002;2:133-142.
 36. Jantsch-Plunger V, Gonczy P, Romano A, et al. CYK-4: a Rho family GTPase activating protein (GAP) required for central spindle formation and cytokinesis. *J Cell Biol*. 2000;149:1391-1404.
 37. Hirose K, Kawashima T, Iwamoto I, Nosaka T, Kitamura T. MgcRacGAP is involved in cytokinesis through associating with mitotic spindle and midbody. *J Biol Chem*. 2001;276:5821-5828.
 38. Van de Putte T, Zwijsen A, Lonnoy O, et al. Mice with a homozygous gene trap vector insertion in MgcRacGAP die during pre-implantation development. *Mech Dev*. 2001;102:33-44.
 39. Mishima M, Kaitna S, Glotzer M. Central spindle assembly and cytokinesis require a kinesin-like protein/RhoGAP complex with microtubule bundling activity. *Dev Cell*. 2002;2:41-54.
 40. Minoshima Y, Kawashima T, Hirose K, et al. Phosphorylation by aurora B converts MgcRacGAP to a RhoGAP during cytokinesis. *Dev Cell*. 2003;4:549-560.
 41. Nosaka T, Kawashima T, Misawa K, Ikuta A, Mui L, Kitamura T. STAT5 as a molecular regulator of proliferation, differentiation and apoptosis in hematopoietic cells. *EMBO J*. 1999;18:4754-4765.
 42. Morita S, Kojima T, Kitamura T. Plat-E: an efficient and stable system for transient packaging of retroviruses. *Gene Ther*. 2000;12:1063-1066.
 43. Miura M, Tamura T, Mikoshiba K. Cell-specific expression of the mouse glial fibrillary acidic protein gene: identification of the cis- and trans-acting promoter elements for astrocyte-specific expression. *J Neuro Chem*. 1990;55:1180-1188.
 44. Simon AR, Vikis HG, Stewart S, Fanburg BL, Cochran BH, Guan K. Regulation of STAT3 by direct binding to the Rac1 GTPase. *Science*. 2000;290:144-147.
 45. Dorseuil O, Gacon G. Signal transduction by Rac small G proteins in phagocytes [in French]. *C R Seances Soc Biol Fil*. 1997;191:237-246.
 46. Roberts AW, Kim C, Zhen L, et al. Deficiency of the hematopoietic cell-specific Rho family GTPase Rac2 is characterized by abnormalities in neutrophil function and host defense. *Immunity*. 1999;10:183-196.
 47. Abe J, Berk BC. Fyn and JAK2 mediate Ras activation by reactive oxygen species. *J Biol Chem*. 1999;274:21003-21010.
 48. Boguski MS, McCormick F. Proteins regulating Ras and its relatives. *Nature*. 1993;366:643-654.
 49. Lamarche N, Hall A. GAPs for rho-related GTPases. *Trends Genet*. 1994;10:436-440.
 50. Kozma R, Ahmed S, Best A, Lim L. The Ras-related protein Cdc42Hs and bradykinin promote formation of peripheral actin microspikes and filopodia in Swiss 3T3 fibroblasts. *Mol Cell Biol*. 1995;15:1942-1952.
 51. Paulssen RH, Woodson J, Liu Z, Ross EM. Carboxyl-terminal fragments of phospholipase C-beta1 with intrinsic Gq GTPase-activating protein (GAP) activity. *J Biol Chem*. 1996;271:26622-26629.
 52. Faruqi TR, Gomez D, Bustelo XR, Barsagi D, Reich NC. Rac1 mediates STAT3 activation by autocrine IL-6. *Proc Natl Acad Sci U S A*. 2001;98:9014-9019.
 53. Pelletier S, Duhamel F, Coulombe P, Popoff MR, Meloche S. Rho family GTPases are required for activation of Jak/STAT signaling by G protein-coupled receptors. *Mol Cell Biol*. 2003;23:1316-1333.
 54. Sundaresan M, Yu ZX, Ferransai VJ, et al. Regulation of reactive-oxygen-species generation in fibroblasts by Rac1. *Biochem J*. 1996;318:379-382.
 55. Babior BM. NADPH oxidase: an update. *Blood*. 1999;93:1464-1476.
 56. Gu Y, Byrne MC, Paranaivana NC, et al. Rac2, a hematopoiesis-specific Rho GTPase, specifically regulates mast cell protease gene expression in bone marrow-derived mast cells. *Mol Cell Biol*. 2002;22:7645-7657.
 57. Tatsumoto T, Xie X, Blumenthal R, Okamoto I, Miki T. Human ECT2 is an exchange factor for Rho GTPases, phosphorylated in G2/M phases, and involved in cytokinesis. *J Cell Biol*. 1999;147:921-928.
 58. Somers WG, Saint R. A RhoGEF and Rho family GTPase-activating protein complex links the contractile ring to cortical microtubules at the onset of cytokinesis. *Dev Cell*. 2003;4:29-39.

STEM CELLS®

Rapid Communication

Human Placenta-Derived Cells Have Mesenchymal Stem/Progenitor Cell Potential

YUMI FUKUCHI, HIDEAKI NAKAJIMA, DAISUKE SUGIYAMA,
IMIKO HIROSE, TOSHIO KITAMURA, KOHICHIRO TSUJI

Division of Cellular Therapy, The Advanced Clinical Research Center,
Institute of Medical Science, The University of Tokyo, Japan

Key Words. Human placenta • Placenta-derived cells • Mesenchymal stem/progenitor cells • Cell culture

ABSTRACT

Mesenchymal stem/progenitor cells (MSCs) are widely distributed in a variety of tissues in the adult human body (e.g., bone marrow [BM], kidney, lung, and liver). These cells are also present in the fetal environment (e.g., blood, liver, BM, and kidney). However, MSCs are a rare population in these tissues. Here we tried to identify cells with MSC-like potency in human placenta. We isolated adherent cells from trypsin-digested term placentas and established two clones by limiting dilution. We examined these cells for morphology, surface markers, gene expression patterns, and differentiation potential and found that they

expressed several stem cell markers, hematopoietic/endothelial cell-related genes, and organ-specific genes, as determined by reverse transcription-polymerase chain reaction and fluorescence-activated cell sorter analysis. They also showed osteogenic and adipogenic differentiation potentials under appropriate conditions. We suggest that placenta-derived cells have multilineage differentiation potential similar to MSCs in terms of morphology, cell-surface antigen expression, and gene expression patterns. The placenta may prove to be a useful source of MSCs. *Stem Cells* 2004;22:649-658

INTRODUCTION

Multipotential mesenchymal stem/progenitor cells (MSCs) can be induced to differentiate into bone, adipose, cartilage, muscle, and endothelium if these cells are cultured under specific permissive conditions [1, 2]. In rodents, a specific type of MSC (termed multipotent adult progenitor cell) can be isolated from bone marrow (BM) and contributes to most somatic cell types when injected into early blastocysts at the single-cell level [3]. Because MSCs have unique immunologic characteristics that suppress lymphocyte proliferation in vitro and prolong skin graft survival in vivo [4], persist-

ence in a xenogeneic environment is favored [1]. With such multiple differentiation capacities and unique immunoregulatory features plus self-renew potential [5], MSCs show promise as a possible therapeutic agent. Data from preclinical transplantation studies suggested that MSC infusions not only prevent the occurrence of graft failure but also have immunomodulatory effects [6].

MSCs are a rare population (approximately 0.001%–0.01%) of adult human BM [7]. Moreover, numbers of BM MSCs significantly decrease with age [8]. MSCs are also relatively few in adult peripheral blood [9] and in term cord

Correspondence: Yumi Fukuchi, Ph.D., Division of Cellular Therapy, The Advanced Clinical Research Center, Institute of Medical Science, The University of Tokyo, 4-6-1 Shirokanedai, Minato-ku, Tokyo 108-8639, Japan. Telephone: 81-3-5449-5759; Fax: 81-3-5449-5453; e-mail: yfukuchi@ims.u-tokyo.ac.jp Received June 6, 2003; accepted for publication March 23, 2004. ©AlphaMedPress 1066-5099/2004/\$12.00/0

STEM CELLS 2004;22:649-658 www.StemCells.com

blood [10]. A recent study showed that the population of MSC-like cells exists within the umbilical vein endothelial/subendothelial layer [11]. Furthermore, MSCs are present in fetal organs, such as liver, BM, and kidney, and circulate in the blood of preterm fetuses [10, 12, 13]. However, fetal samples can be difficult to procure, and term cord blood compared with preterm is a poor source of MSCs [10–12]. Such being the case, searching for appropriate sources, avoiding ethical issues, and establishing suitable culture systems are a challenge.

In this study, we evaluated the possibility that MSCs or cells with MSC-like potency are present in the human term placenta, and we obtained evidence that cells with the phenotype of MSCs exist in this tissue.

MATERIALS AND METHODS

Isolation and Culture of Placenta-Derived Cells

Term placentas ($n = 57$; clinically normal pregnancies, caesarean section) were collected after obtaining written informed consent from donors to the Tokyo Cord Blood Bank.

The internal area (approximately 1 cm^3) of central placenta lobules was minced, hemolyzed, trypsinized (37°C for 5 minutes), and finally prepared in both single-cell suspensions and small digested residues. These samples were cultured with α -minimum essential medium (MEM; Sigma-Aldrich Co., St. Louis, <http://www.sigmaaldrich.com>) and supplemented with 15% fetal bovine serum (FBS; HyClone Laboratories, Logan, UT, <http://www.hyclone.com>), 100 U/ml penicillin, and 100 $\mu\text{g/ml}$ streptomycin (Invitrogen, Paisley, U.K., <http://www.invitrogen.com>). Cultures were maintained at 37°C in a humidified atmosphere with 5% CO_2 . Three to 5 days after initiating incubation, the small digested residues were removed and the culture was continued. Approximately 3 to 4 weeks later, there were some colonies that contained 50 or more fibroblast-like cells that were more than 50% confluent; they were then trypsinized using 0.05% trypsin (Invitrogen) and replated at a 1:4 dilution. Under the same conditions, placenta-derived cells were continued to culture.

Fluorescence In Situ Hybridization Analysis

Human X/Y chromosomes of placenta-derived cells (male, $n = 3$; female, $n = 3$; passages two and three) were cultured on silica-coating slides and examined using CEP X/Y DNA probe kits (Vysis, Inc., Downers Grove, IL, <http://www.vysis.com>) according to the manufacturer's instructions. The slides were scanned under a fluorescence microscope using a

rhodamine/fluorescein isothiocyanate (FITC) filter for X/Y chromosomes and a UV filter for 4',6-diamidino-2'-phenylindole dihydrochloride-stained cell nuclei.

Fluorescence-Activated Cell Sorter Analysis

Frozen and thawed placenta-derived cells ($n = 3$, passages 9–12) were trypsinized and incubated with medium containing 15% FBS-2 mM EDTA (pH 8.0) for 3 hours. Next the cells were stained with anti-human specific antibodies CD45-phycoerythrin (PE), CD31-PE, CD54-PE, CD29-FITC or CD29-PE, CD44-FITC or CD44-PE (BD Pharmingen, San Diego, <http://www.bdbiosciences.com>), AC133/1-PE (Miltenyi Biotec GmbH, Germany, <http://www.miltenyibiotec.com>), or PE- or FITC-conjugated isotype control (BD Biosciences, San Jose, CA, <http://www.bd.com>). After staining, cells were analyzed using fluorescence-activated cell sorter (FACS) Calibur flow cytometry (Becton, Dickinson, Mountain View, CA).

RNA Extraction and Reverse Transcription-Polymerase Chain Reaction

Total RNA from 10^5 – 10^6 placenta-derived cells ($n = 15$, passages 2–18, including frozen and thawed samples) was isolated using ISOGEN (Nippon Gene, Tokyo). RNA extracts were treated with deoxyribonuclease I (Amplification Grade, Invitrogen) for digesting contaminated genomic DNA.

Reverse transcription (RT) reactions were carried out on 1 μg of total RNA using the ThermoScript™ RT-polymerase chain reaction (PCR) system (Invitrogen), and 40 cycles of PCR were run using the Platinum PCR SuperMix (Invitrogen) according to the manufacturer's instructions. Evaluation of all PCRs was estimated using appropriate human tissue RNA (Clontech Laboratories, Inc., Palo Alto, CA, <http://www.clontech.com>), human BM-derived MSCs (Bio Whittaker, Inc., Walkersville, MD), and human cell lines [14, 15]. cDNA synthesis and genomic DNA contamination were examined using HOXB4 primers, which give products of 268 bp and 1.1 kb when amplifying cDNA and genomic DNA, respectively. Human-specific primers used were as follows: Oct-4 (866 bp), CCGCCGTATGAGTTCTGTGG/AGAGTGGTGACAGAGACAGG; Rex-1 (449 bp), ATGGCTATGTGTGCTATGAGC/CCTCAACTTCTAGTGCATCC; HOXB4 (268 bp), CTACCCCTGGATGCCCAAAG/CGAGCGGATCTTGGTGTGG; CBF β (300 bp), TCGTGCCCGACCAGAGAAGC/TCAGAATCATGGGAGCCTTC; β 2-microglobulin (341 bp), GAGTGCTGTCTCATGTTTG/TAACCACAACCATGCCTTAC; GATA-2 and Tie-2 [16]; TAL-1 [17]; CD34, AC133, *flk-1*, myogenin,

nestin, and α -1-fetoprotein [18]; flt-1 [19]; Nkx2.5 and GATA-4 [20]; renin and albumin [21]; GFAP [22]; and amy-lase and insulin [23].

Differentiation Studies

Passage 2 through 11 placenta-derived cells, including frozen and thawed samples ($n = 8$), were cultured either in an osteogenic (0.1 μ M dexamethasone, 10 mM β -glycerol phosphate, 50 μ M ascorbate) or adipogenic (1 μ M dexamethasone, 5 μ g/ml insulin, 0.5 mM isobutylmethylxanthine, 60 μ M indomethacin) medium (all chemicals from Sigma) [10] on two-well Permaxox slides (Nalge Nunc International, Naperville, IL). After 2 weeks, osteogenic differentiation was evaluated after 1% Alizarin Red S (Sigma) staining, and adipogenic differentiation was assessed using Oil Red O (Sigma) staining [2].

Subcloning and Characterization of Placenta-Derived Clones

The MSCV-IRES-GFP retroviral plasmid was transfected in PLAT-A packaging cells. Retroviral supernatants were collected and infected in No. 40 placenta-derived cells (passage five). The green fluorescent protein (GFP)-positive cells (passage seven) were sorted by FACS Vantage flow cytometry (Becton, Dickinson) and then subcultured at 5 or 10 cells per well (passage nine). After subcloning, we selected single retroviral-inserted subclones by Southern blot analysis using a GFP cDNA probe. Two clones were obtained, and then we carried out a FACS and RT-PCR analysis and differentiation studies for characterization of these clones.

RESULTS

Characterization of Placenta-Derived Cells

Searching for alternative sources of MSCs, we attempted to prepare human term placentas and isolated fibroblast-like cells from every placenta isolation ($n = 57$; Fig. 1). In a single-cell suspension culture of the isolated placenta, cells firstly formed colony-forming unit fibroblast (CFU-F)-like colonies (Figs. 1A, b). On the other hand, in the culture of small trypsin-digested residues of placenta, cells began to migrate and proliferate (data not shown). After the first passage, cells from both samples expanded in the same monolayer manner (Fig. 1A, a-c). Cord blood (CB) is a rich source of hematopoietic stem cells and MSCs, and the term placenta contains much CB, primarily adherent cells derived from freshly isolated CB mononuclear cells ($n = 77$). However, CBs were obtained (after receiving the informed consent

from Kiyosenomori Hospital, Tokyo) but did not survive in α -MEM containing 15% FBS. To determine whether these cells were from maternal or fetal parts of the placenta, we did a fluorescence in situ hybridization analysis using X- and Y-probes. These cells were positive for X- and Y-signals, indicating that they were from a fetal part of the placenta (Fig. 1B). The placenta-derived cells were classified into two groups according to growth characteristics; one could proliferate more than 20 passages (Fig. 1C, Nos. 40 and 29), and the other went into replicative senescence between 10 and 20 passages (Fig. 1C, Nos. 41 and 44). The former type had a small and homogeneous morphology, but the latter type was of a bigger shape than the former. We also examined the surface marker profile of the above three representative placenta-derived cell lines using FACS, and these three lines had a similar phenotype, as follows: CD45^{low}CD31⁻AC133⁻CD54⁺CD29⁺CD44⁺ (Fig. 1D), which closely resembles the phenotypes of BM-derived and CB-derived MSCs [2, 7, 10, 24].

Gene Expression Patterns of Placenta-Derived Cells

For a closer study of placenta-derived cells, we did a RT-PCR analysis for various genes, including stem cell markers, hematopoietic/endothelial cell-related genes, and organ-specific genes. The placenta-derived cells expressed many of the genes derived from mesoderm, ectoderm, and endoderm (Fig. 2). Additionally, expression patterns of stem cell markers and hematopoietic/endothelial cell-related genes in placenta-derived cells were similar to those of human BM (hBM)-derived MSCs (Fig. 2, lane 2).

Differentiation Potential of Placenta-Derived Cells

To estimate the potential to differentiate into osteoblasts and adipocytes, the placenta-derived cells were cultured in osteogenic or adipogenic medium. At the end of the induction periods, most of the cells were Alizarin Red S-positive (Figs. 3B, 3C) or Oil Red O-positive (Figs. 3E, 3F), indicating differentiation to osteoblasts or adipocytes, respectively. In contrast, cells cultured with regular medium were not significantly stained (Figs. 3A, 3D). Such data indicate that the placenta-derived cells had bidirectional differentiation potency.

Subcloning of Placenta-Derived Cells

The placenta-derived cells used in the above experiments are obviously heterogeneous and may be a mixture of progenitors that can differentiate into specific lineages. To

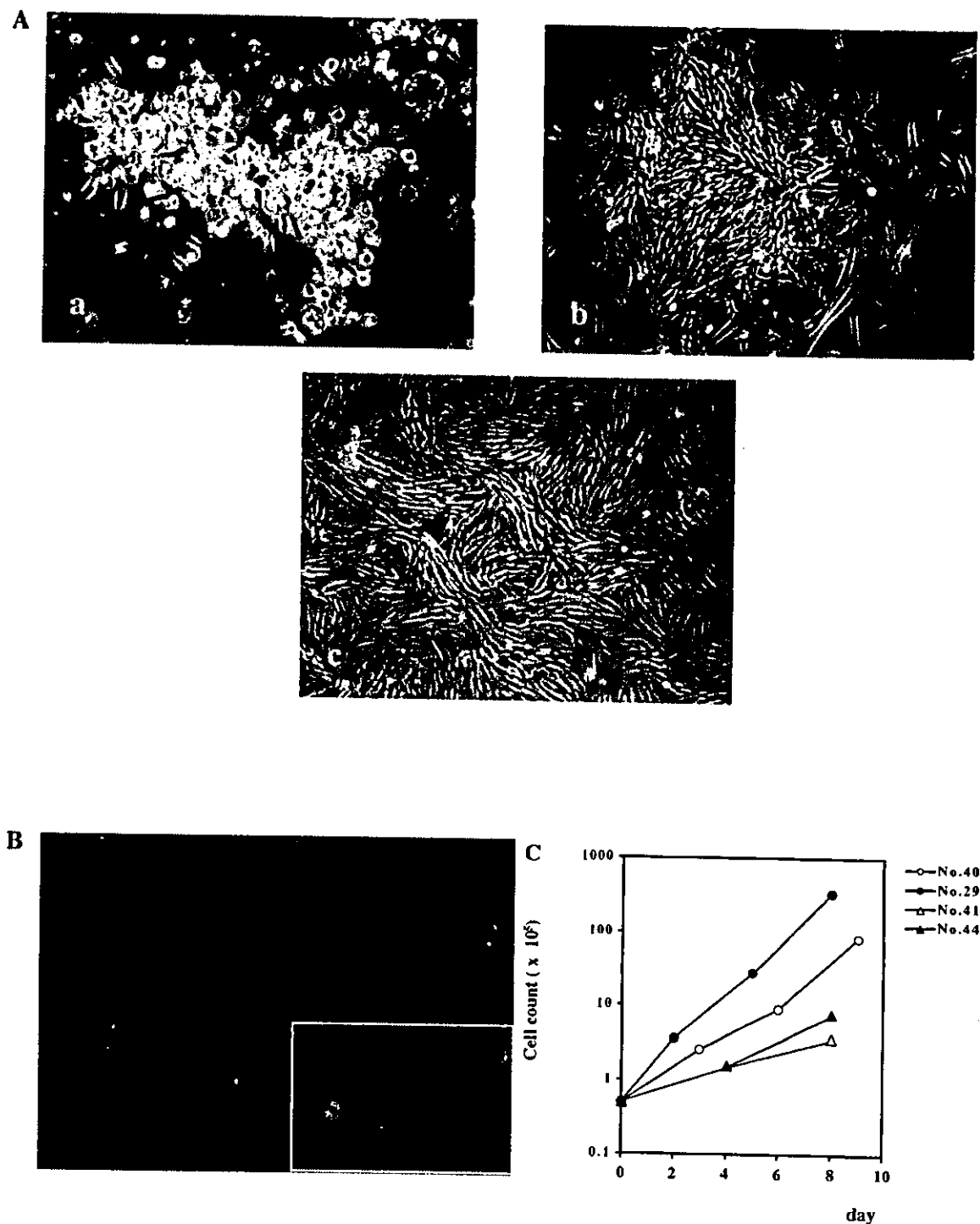


Figure 1. Isolation and characterization of placenta-derived cells. (A): Morphology of placenta-derived cells. Cells from a single-cell suspension easily expanded through the formation of colony-forming unit fibroblast-like colonies. a: 10 days after isolation ($\times 100$ magnification); b: 3 weeks after isolation ($\times 40$ magnification); c: 6 weeks after isolation (passage 3; $\times 40$ magnification). (B): Fluorescence in situ hybridization analysis for human X/Y chromosomes. Cells from male placenta have Y-positive (green) and X-positive (orange) signals. (C): Growth curve of placenta-derived cells. Frozen and thawed cells ($n = 4$, started at passage six or seven) were seeded at 0.5×10^5 cells per well and cultured until 90% confluence was reached. These cells were resuspended, enumerated, and reseeded at the same density for 10 days. (D): Immunophenotype of placenta-derived cells. Cells were stained with phycoerythrin-conjugated or fluorescein isothiocyanate-conjugated antibodies against CD45, CD31, AC133, CD54, CD29, CD44, or immunoglobulin isotype control antibodies. Cells were analyzed using fluorescence-activated cell sorter Calibur. Individual placenta-derived cells were given serial numbers of placenta isolation. Representative samples were used for these figures. (Figure 1D continued on next page.)

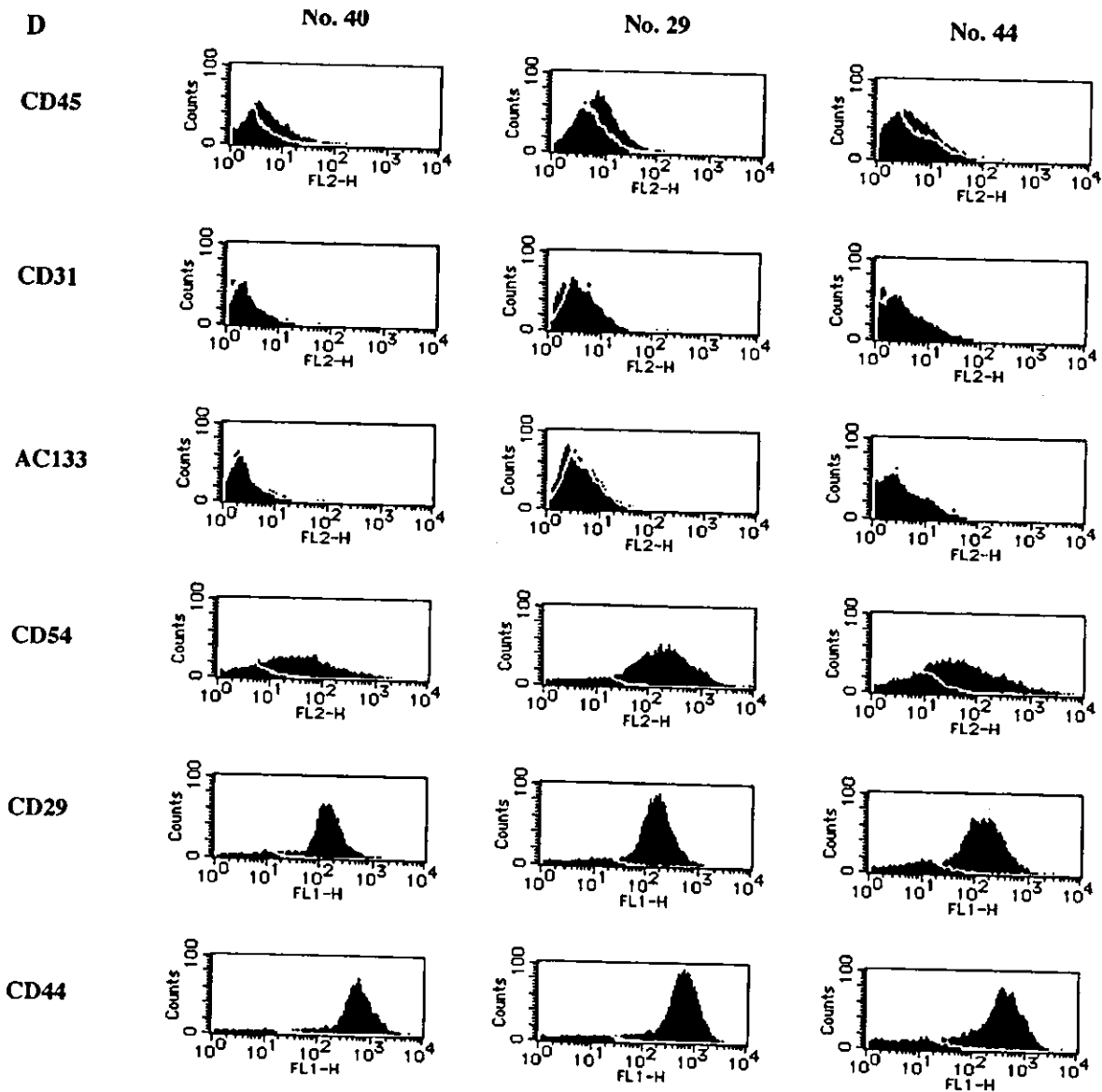


Figure 1 (continued).

exclude this possibility, we attempted to subclone No. 40 placenta-derived cells showing the human MSC (hMSC)-like gene expression pattern using RT-PCR (Fig. 2, lanes 2 and 7). We established two clones, B2 and F4 (Fig. 4A, lanes 1 and 9), which retained almost all of the phenotypes of their parental cells; surface marker expression ($CD45^{low}CD31^{-}AC133^{-}CD54^{+}CD29^{+}CD44^{+}$), gene expression patterns, and differentiation potential (Figs. 4B–4D versus Figs. 1–3). Moreover, these phenotypes were similar to those of other placenta-derived cell lines. Such data suggest that although the placenta-derived cells are considered to be polyclonal, most of the clones are similar in gene-expression profiles and

retain the differentiation capacity to osteoblasts and adipocytes.

DISCUSSION

In this study, we successfully isolated placenta-derived cells from human term placentas ($n = 57$) and then characterized morphology, cell-surface antigens, gene expression patterns, and differentiation capacity of these cells. Results of RT-PCR analysis of 15 individual placenta-derived cells showed that the expression patterns of seven genes (HOXB4, CD34, AC133, flk-1, Tie-2, GATA-4, and myogenin) varied but expressions of 14 other genes were quite similar (Fig. 2

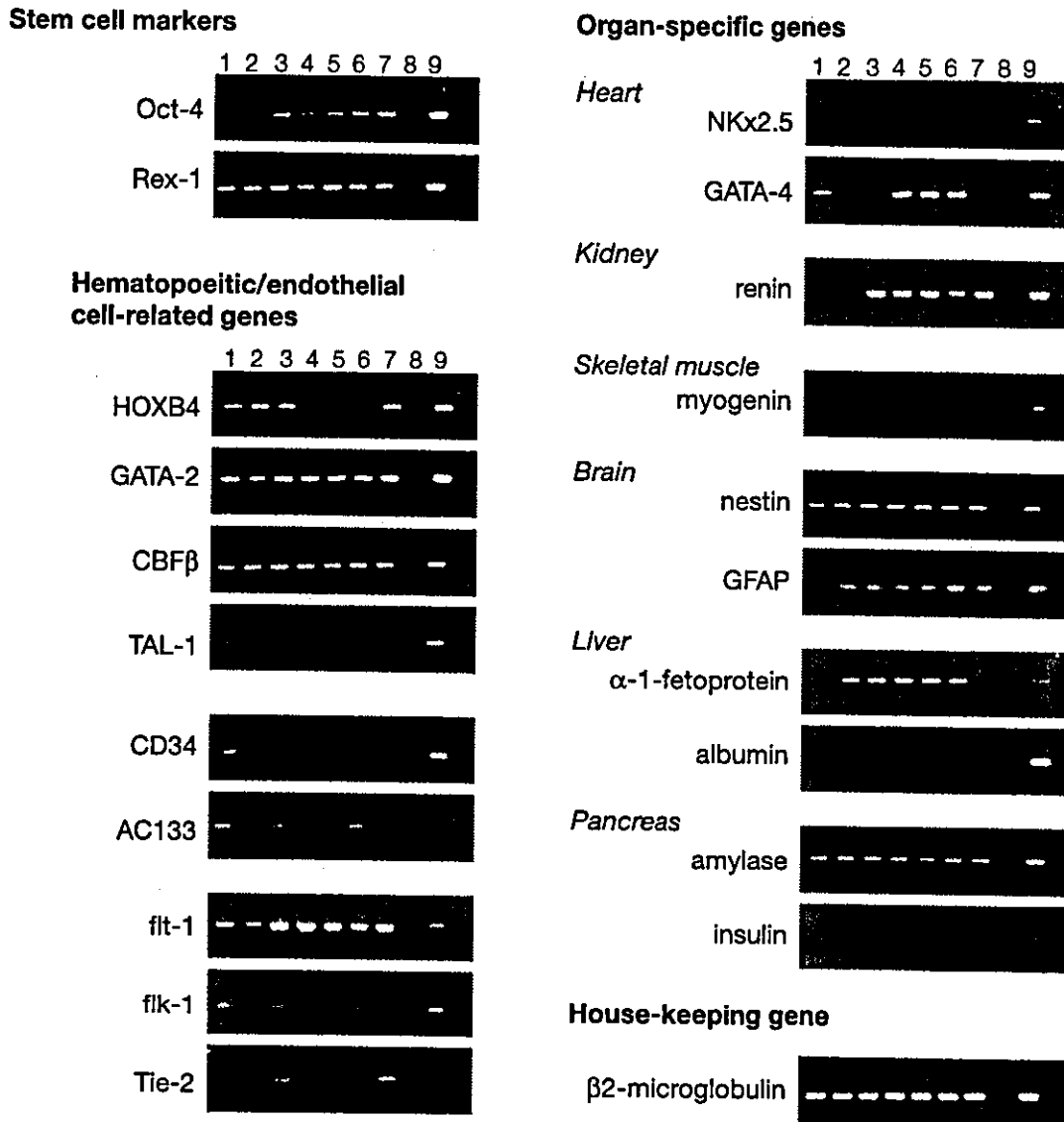


Figure 2. Gene expression patterns of placenta-derived cells. Placenta-derived cells were characterized using reverse transcription-polymerase chain reaction. Samples are as follows: lane 1, noncultured placenta (trypsin-digested residue); lane 2, human bone marrow-derived mesenchymal stem/progenitor cells; lanes 3–7, placenta (Nos. 29, 41, 42, 44, and 40)-derived cells; lane 8, reagent control; lane 9, positive control (i.e., Oct-4, Rex-1, HOXB4, and β 2-microglobulin were used for EoL-3. GATA-2, CBF β , TAL-1, CD34, AC133, flk-1, and flt-1 were used for TF-1. NKx2.5 and GATA-4 were used for human heart RNA. Renin and myogenin were used for human kidney RNA and skeletal muscle RNA, respectively. Nestin and GFAP were used for human brain RNA. α -1-fetoprotein and albumin were used for human liver RNA. Amylase and insulin were used for human pancreas RNA). In this figure, we took up the data from the five representative placenta-derived cells, and each of placenta-derived cells was shown by serial numbers of placenta isolation.

shows evidence of six placenta-derived cells; nine are not shown). These expression patterns resemble those of hBM-derived MSCs, except for renin and flt-1 (Fig. 2, lane 2). Comparison of the two types of placenta-derived cells with distinct growth characteristics (one that propagates more than 20 passages [Fig. 1C, Nos. 40 and 29] and the other with growth limitation [Nos. 41, 42, and 44]) showed that the expressions of HOXB4, CD34, Tie-2, and GATA-4 were different among these groups. The former more resembled the

hBM-derived MSCs for gene expression patterns (Fig. 2). Collectively, these results indicate that the placenta-derived cells have MSC-like gene expression patterns. In addition, they showed a differentiation capacity toward both osteoblasts and adipocytes (Fig. 3), suggesting that these cells have MSC-like differentiation potential.

Because the original culture of 57 placenta-derived cell lines should be a mixture of a variety of cell types, we attempted to subclone these cells to do a detailed analysis.

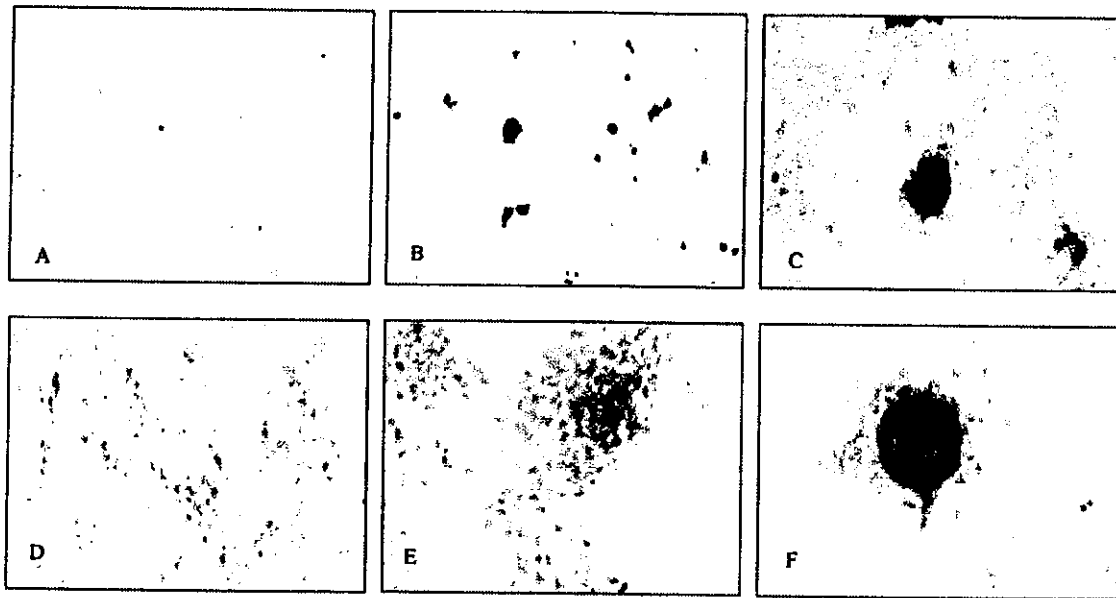


Figure 3. Differentiation potential of placenta-derived cells. After a 2-week culture in osteogenic (B, C) or adipogenic (E, F) medium or regular medium (A, D), each of the placenta-derived cells was evaluated for osteogenic or adipogenic differentiation using specific staining and hematoxylin counterstaining. Magnification: A, B, D, E, $\times 40$; C, F, $\times 100$. A representative sample was used for this figure.

Two established clones retained almost all of the phenotypes of parental No. 40 placenta-derived cells, including morphology, cell-surface populations, gene expression patterns, and differentiation capacity. However, these clones also had some differences in mRNA expression, such as CD34 and α -1-fetoprotein. These genes were upregulated compared with the parent mixture cells (Figs. 2, 4C). In some reports, small proportions of hMSCs expressed low levels of CD34 [6, 25]. Further experiments are required to determine the meaning of expressions of these genes.

Rex-1 is known to be important for maintaining undifferentiated embryonic stem cells [26, 27]. However, the role of this gene in MSCs is not clear. The result of RT-PCR analysis showed that Rex-1 is expressed in both BM-derived MSCs and placenta-derived cells (Fig. 2) but not in the two clones (Fig. 4C). Analysis of parental placenta-derived cells at various time points during passages (passages 3, 5, 9, and 18 for original cells; passages 13 and 26 for GFP-labeled mixture cells) using RT-PCR showed that only Rex-1 expression switched from positive (before passage 5, Fig. 2) to negative (after passage 9; data not shown). Additional analysis is required to know the role of Rex-1 in placenta-derived cells.

Interestingly, cell-surface markers analyzed using FACS revealed that the placenta-derived mixture cells and clones had the CD45^{low}CD31⁻AC133⁻CD54⁺CD29⁺CD44⁺ phenotype (Figs. 1D, 4B), and the expression of CD45 and AC133 antigens differed from MSCs derived from other sources [2,

7, 10, 24]. As for the expression of AC133, the results were negative with FACS yet positive with RT-PCR analysis. This contradictory finding may be due to a damaged AC133 epitope by trypsin treatment of the cells. As for the expression of CD45, some reports showed that unprocessed or fresh MSCs were CD45^{med,low}, whereas cultured MSCs and more mature cells were CD45⁻ [24, 28]. However, as our results showed, the expression of CD45 was low during passages. The CD45^{low} phenotype might be one of the specific characteristics of the placenta-derived cells.

This study showed that the placenta-derived MSC-like cells could be easily isolated and expanded without morphological and characteristic changes in medium supplemented only with FBS. Therefore, the placenta may prove to be an attractive and rich source of MSCs. Further studies are required to better understand the precise nature of placenta-derived cells and to explore their potential clinical applications.

ACKNOWLEDGMENTS

We thank Drs. T. A. Takahashi and N. Watanabe (Division of Cell Processing, Institute of Medical Science, The University of Tokyo, Japan) for significant advice on these placenta-derived cells; Dr. Y. Koshino and Ms. M. Ito (Division of Cellular Therapy, Institute of Medical Science, The University of Tokyo, Japan) for advice and technical support; and Drs. H. Funabiki and S. Akutsu (Kiyosonomori Hospital, Japan) for assistance with cord blood collections.

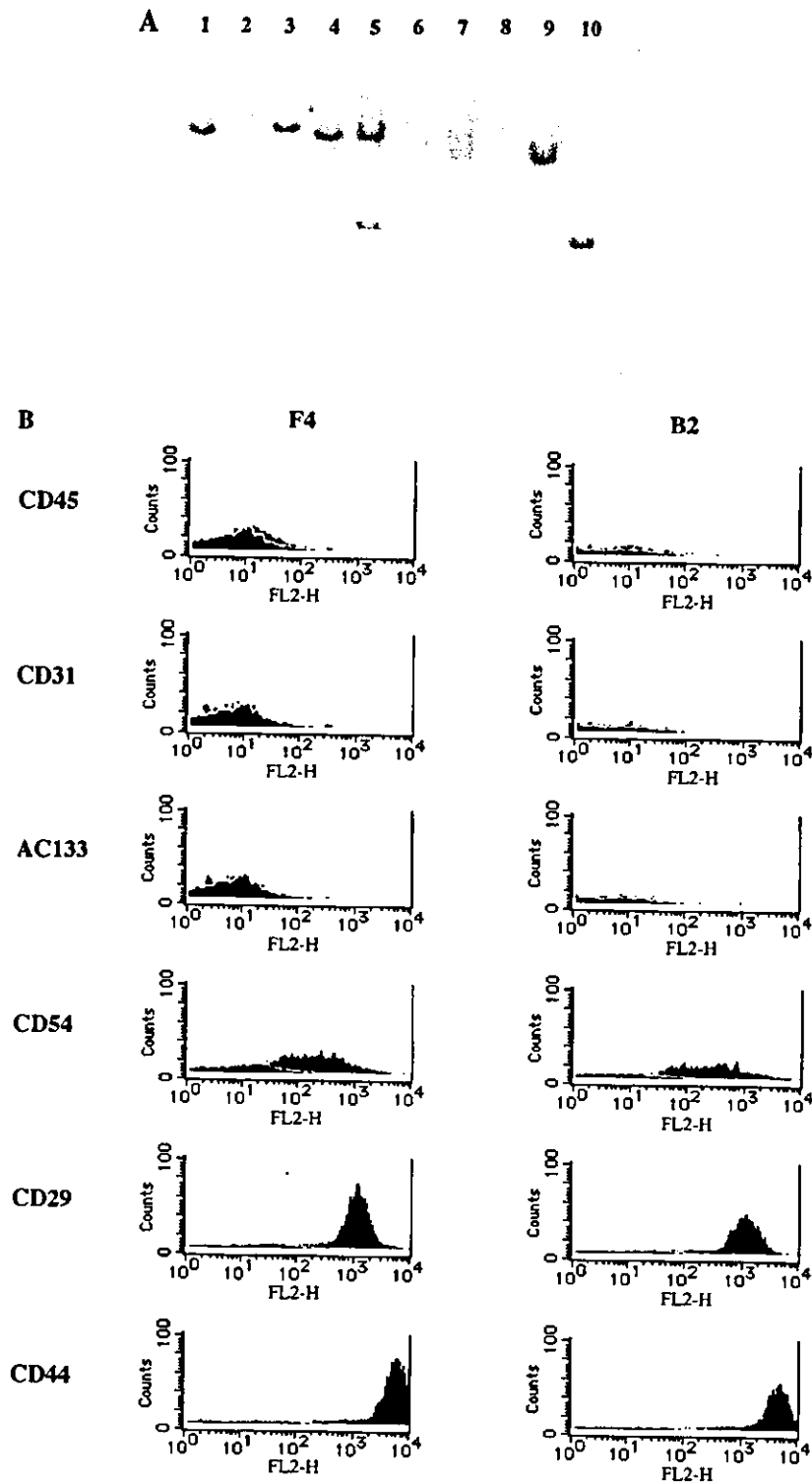


Figure 4. Establishment and characterization of two clones from No. 40 placenta-derived cells. (A): Establishment of placenta-derived clones. No. 40 placenta-derived cells were transduced with MSCV-IRES-GFP retrovirus, and green fluorescent protein (GFP)-positive population was sorted by fluorescence-activated cell sorting, then replated onto a 96-well dish at 5 or 10 cells per well and expanded. DNAs from these GFP-positive No. 40 placenta-derived subclones were digested overnight with BamHI (cut only once in the MSCV-IRES-GFP plasmid), and fragments were separated by electrophoresis and probed with a 32 P-labeled GFP cDNA probe. Samples are as follows for lanes 1-6, 8, and 9: subclones B2, B4, D2, D3, E4, G3, F1, and F4, respectively. These subclones were obtained from subcloning of five cells per well. Lanes 7 and 10, subclones E4 and G4. (Figure 4C and D continued on next page.) (Figure 4C and D continued on next page.)

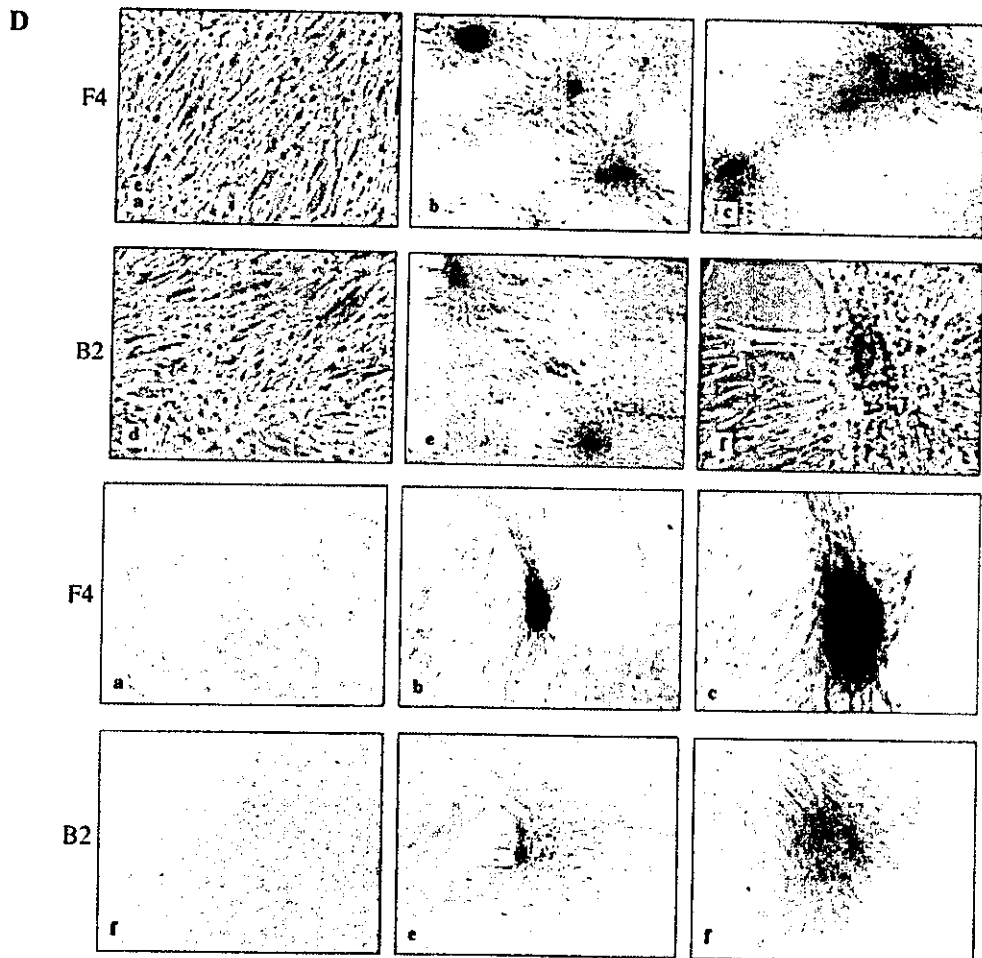
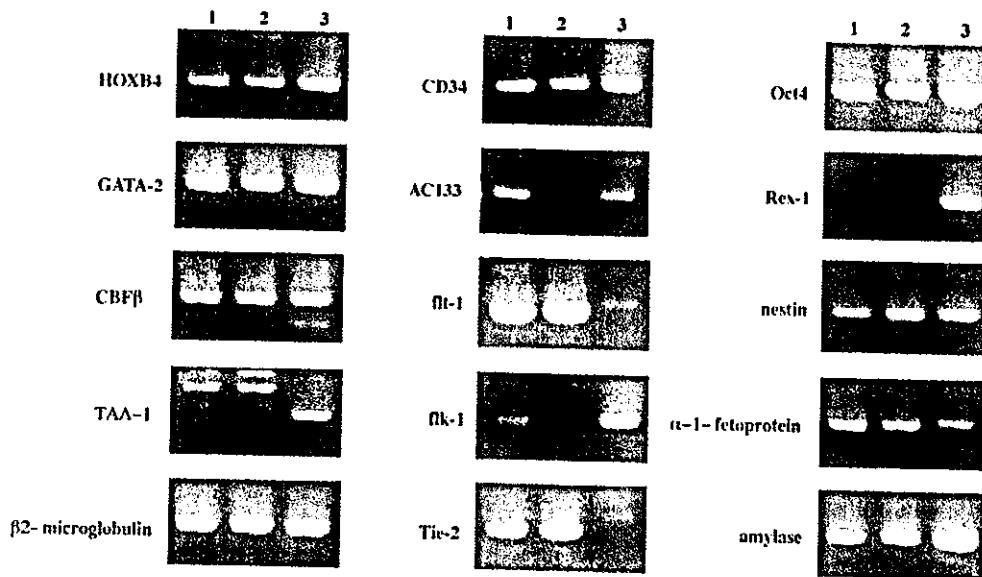


Figure 4 (continued). These were obtained from subcloning of 10 cells per well. Subclones B2 (lane 1) and F4 (lane 9) had a single retroviral insert. (B): Immunophenotype of clones. Clones F4 and B2 were stained with phycoerythrin-conjugated antibodies against CD45, CD31, AC133, CD54, CD29, and CD44 or immunoglobulin isotype control antibodies then analyzed by fluorescence-activated cell sorter Calibur. (C): Gene expression patterns of clones. Clones F4 and B2 were characterized by reverse transcription-polymerase chain reaction analysis. Samples are as follows: lane 1, clone F4; lane 2, clone B2; lane 3, positive control (same positive controls were used in Fig. 2). (D): Differentiation potential of clones. Clones F4 and B2 were cultured in osteogenic (b, c, e, f), adipogenic (h, i, k, l), or regular medium (a, d, g, j) for 2 weeks. After the culture periods, each of the clones was evaluated for osteogenic or adipogenic differentiation using specific staining and hematoxylin counterstaining. Magnification: a, b, d, e, g, h, j, k, $\times 40$; c, f, i, l, $\times 100$.

REFERENCES

- 1 Liechty KW, MacKenzie TC, Shaaban AF et al. Human mesenchymal stem cells engraft and demonstrate site-specific differentiation after in utero transplantation in sheep. *Nat Med* 2000;6:1282–1286.
- 2 Reyes M, Lund T, Lenvik T et al. Purification and ex vivo expansion of postnatal human marrow mesodermal progenitor cells. *Blood* 2001;98:2615–2625.
- 3 Jiang Y, Jahagirdar BN, Reinhardt RL et al. Pluripotency of mesenchymal stem cells derived from adult marrow. *Nature* 2002;20:1–9.
- 4 Bartholomew A, Sturgen C, Siatskas M et al. Mesenchymal stem cells suppress lymphocyte proliferation in vitro and prolong skin graft survival in vivo. *Exp Hematol* 2002;30:42–48.
- 5 Gerson SL. Mesenchymal stem cells: no longer second class marrow citizens. *Nat Med* 1999;5:262–264.
- 6 Deans RJ, Moseley AB. Mesenchymal stem cells: biology and potential clinical uses. *Exp Hematol* 2000;28:875–884.
- 7 Pittenger MF, Mackay AM, Beck SC et al. Multilineage potential of adult human mesenchymal stem cells. *Science* 1999;284:143–147.
- 8 Rao MS, Mattson MP. Stem cells and aging: expanding the possibilities. *Mech Aging Dev* 2001;122:713–734.
- 9 Zvaifler NJ, Marinova-Mutafchieva L, Adams G et al. Mesenchymal precursor cells in the blood of normal individuals. *Arthritis Res* 2000;2:477–488.
- 10 Erices A, Conget P, Minguell JJ. Mesenchymal progenitor cells in human umbilical cord blood. *Br J Haematol* 2000;109:235–242.
- 11 Romanov YA, Svintsitskaya VA, Smirnov VN. Searching for alternative sources of postnatal human mesenchymal stem cells: candidate MSC-like cells from umbilical cord. *STEM CELLS* 2003;21:105–110.
- 12 Campagnoli C, Roberts IAG, Kumar S et al. Identification of mesenchymal stem/progenitor cells in human first-trimester fetal blood, liver, and bone marrow. *Blood* 2001;98:2396–2402.
- 13 Almeida-Porada G, Shabrawy D, Porada C et al. Differentiative potential of human metanephric mesenchymal cells. *Exp Hematol* 2002;30:1454–1462.
- 14 Kitamura T, Tange T, Terasawa T et al. Establishment and characterization of a unique human cell line that proliferates dependently on GM-CSF, IL-3, or erythropoietin. *J Cell Physiol* 1989;140:323–334.
- 15 Hosoda M, Makino S, Kawabe T et al. Differential regulation of the low affinity Fc receptor for IgE (Fc epsilon R2/CD23) and the IL-2 receptor (Tac/p55) on eosinophilic leukemia cell line (EoL-1 and EoL-3). *J Immunol* 1989;143:147–152.
- 16 Levenberg S, Golub JS, Amit M et al. Endothelial cells derived from human embryonic stem cells. *Proc Natl Acad Sci U S A* 2002;99:4391–4396.
- 17 Kaufman DS, Hanson ET, Lewis RL et al. Hematopoietic colony-forming cells derived from human embryonic stem cells. *Proc Natl Acad Sci U S A* 2001;98:10716–10721.
- 18 Shambloott MJ, Axelman J, Littlefield JW et al. Human embryonic germ cell derivatives express a broad range of developmentally distinct markers and proliferate extensively in vitro. *Proc Natl Acad Sci U S A* 2001;98:113–118.
- 19 Bellamy WT, Richter L, Frutiger Y et al. Expression of vascular endothelial growth factor and its receptors in hematopoietic malignancies. *Cancer Res* 1999;59:728–733.
- 20 Kehat I, Kenyagin-Karsenti D, Snir M et al. Human embryonic stem cells can differentiate into myocytes with structural and functional properties of cardiomyocytes. *J Clin Invest* 2001;108:407–414.
- 21 Schuldiner M, Yanuka O, Itskovitz-Eldor J et al. Effects of eight growth factors on the differentiation of cells derived from human embryonic stem cells. *Proc Natl Acad Sci U S A* 2000;97:11307–11312.
- 22 Vescovi AL, Parati EA, Gritti A et al. Isolation and cloning of multipotential stem cells from the embryonic human CNS and establishment of transplantable human neural stem cell lines by epigenetic stimulation. *Exp Neurol* 1999;156:71–83.
- 23 Zulewski H, Abraham EJ, Gerlach MJ et al. Multipotential nestin-positive stem cells isolated from adult pancreatic islets differentiate ex vivo into pancreatic endocrine, exocrine, and hepatic phenotypes. *Diabetes* 2001;50:521–533.
- 24 Reyes M, Dudek A, Jahagirdar B et al. Origin of endothelial progenitors in human postnatal bone marrow. *J Clin Invest* 2002;109:337–346.
- 25 Deschaseaux F, Gindraux F, Saadi R et al. Direct selection of human bone marrow mesenchymal stem cells using an anti-CD49a antibody reveals their CD45^{med,low} phenotype. *Br J Haematol* 2003;122:506–517.
- 26 Ben-Shushan E, Thompson JR, Gudas LJ et al. Rex-1, a gene encoding a transcription factor expressed in the early embryo, is regulated via Oct-3/4 and Oct-6 binding to an octamer site and a novel protein, Rox-1, binding to an adjacent site. *Mol Cell Biol* 1998;18:1866–1878.
- 27 Niwa H, Miyazaki J, Smith AG. Quantitative expression of Oct-3/4 defines differentiation or self-renewal of ES cells. *Nat Genet* 2000;24:372–376.
- 28 Clark E, Wognum AW, Marciniak R et al. Mesenchymal cell precursors from human bone marrow have a phenotype that is direct from cultured mesenchymal cells and are exclusively present in a small subset of CD45^b SH2⁺ cells. *Blood* 2001;98:85a.